DESIGN AND CFD VALIDATION OF A METHOD OF CHARACTERISTICS CODE FOR SUPERSONIC WIND TUNNELS

A Thesis

by

TREVOR RILEY BLAIR

Submitted to the Office of Graduate and Professional Studies of
Texas A&M University
in partial fulfillment of the requirements for the degree of

MASTER OF SCIENCE

Chair of Committee,	Rodney D. Bowersox
Committee Members,	Edward White
	Waruna Kulatilaka
Head of Department,	Srinivas Vadali

May 2021

Major Subject: Aerospace Engineering

ABSTRACT

Supersonic wind tunnels are a critically important engineering tool used to make aerodynamic discoveries and technological advancements in the high speed flight regime. Great care must be taken when designing the nozzle for a supersonic wind tunnel, as the quality of data produced throughout the lifetime of the facility depends on the quality of the nozzle contour. A nozzle design code was developed to expand the capabilities of the National Aerothermochemistry and Hypersonics Labratory, permitting the timely creation of new nozzles that feature elongated flow expansion near the throat. The foundation of the code is a hyperbolic partial differential equation governing irrotational, inviscid, adiabatic flow inside a nozzle, derived from governing principles of gas dynamics. This equation was reduced, through the method of characteristics, to a system of ordinary differential equations which are solved along characteristic lines with the modified Euler predictor-corrector method for flow parameters inside of the diverging section of the nozzle. The code generates a nozzle based on the user's desired throat height, radius of curvature of the circular throat region, turning angle of the circular region, and Mach number. The code outputs a fully defined nozzle contour. Computational fluid dynamics simulations were performed for several designed contours to validate the code. A grid convergence study was performed, followed by a study of the effect of the initial-value line Mach number input on nozzle performance. Simulations of selected nozzles were performed to quantify the code's performance, including a short and long converging-diverging nozzle to demonstrate the unique capability of the code. Aerodynamically-uniform flow was produced for all test cases, which resulted in a successful MOC code. A recommendation was made to couple a CFD solver with an optimization algorithm to produce hypersonic nozzles contours corrected for viscous effects induced at higher Mach numbers.

ACKNOWLEDGMENTS

There are countless individuals who have supported and aided me during my graduate work here at Texas A&M. Although I couldn't possibly name all of them, I would like to acknowledge the contributions of some special people.

I would first like to thank Dr. Bowersox for all of the guidance he has provided me throughout my graduate career. He accepted me as a graduate student when I decided to pursue graduate studies during my senior year of my undergraduate degree, and I am extremely grateful for the opportunities he has provided for me. I would also like to thank Dr. White and Dr. Kulatilaka for serving on my thesis committee.

I couldn't have completed my studies without the constant support of the students at the NAL. I'd think that I drove them crazy talking about how my code wouldn't work, but somehow they listened and supported me through the issues and the breakthroughs. I would like to give a special shoutout to Joe Carlson, who in one day helped me break through a month's worth of troubleshooting. Special thanks goes to Rebecca Marianno, Cecil Rhodes, and Colleen Leatherman for their administrative skills and keeping the NAL running even through a pandemic.

I would like to acknowledge my parents for their unwavering support for my studies, nurturing a love for science and math from a young age and encouraging me throughout my undergraduate and graduate career. I wouldn't be here today without their love and time sacrificed for me.

Lastly, I would like to thank my wife Allison for supporting me in the process of writing this thesis. Your constant support and encouragement sustained me through all of the stress and trials this work has caused, and I am eternally grateful for the love you've given me.

CONTRIBUTORS AND FUNDING SOURCES

Contributors

This work was supported by a thesis committee consisting of Dr. Rodney Bowersox (advisor) and Dr. Edward White of the Department of Aerospace Engineering, and Dr. Waruna Kulatilaka of the Department of Mechanical Engineering.

All work conducted for the thesis was completed by the student independently.

Funding Sources

The author gratefully acknowledges support for this work in part from a grant from the Department of Defense Office of the Under Secretary of Defense (Vannevar Bush Faculty Fellowship Grant N00014-18-1-3020). Its contents are solely the responsibility of the author and do not necessarily represent the official views of the Department of Defense Office of the Under Secretary of Defense.

NOMENCLATURE

Acronyms & Abbreviations

ODE	Ordinary Differential Equation
PDE	Partial Differential Equation
MOC	Method Of Characteristics
CFD	Computational Fluid Dynamics
HXT	Hypervelocity Expansion Tunnel

Parameters & Variables

ρ	Density
∇	Vector differential operator
$\overrightarrow{V}$	Velocity vector
a	Speed of sound
p	Pressure
V	Scalar velocity
δ	Kroneker delta, 1 for axisymmetric flow, 0 for planar flow
u	Flow velocity along x-direction in Cartesian coordinate system
v	Flow velocity along y-direction in Cartesian coordinate system
σ	Parameter used in method of characteristics
λ	Slope of characteristic curve
θ	Angle of tangential flow along a streamline

α	Mach angle
M	Mach number
ρ_{td}	Radius of curvature of downstream throat contour

TABLE OF CONTENTS

Page

LIST OF FIGURES

1. INTRODUCTION

1.1 Motivation

When designing a flight vehicle, building and flying the vehicle is the most accurate way to test performance parameters during the design phase. This approach can be costly, so wind tunnels are often utilized in the design and testing phase of flight vehicles. Additionally, wind tunnels can test phenomena that are not easily measured in real flight. A critical high speed wind tunnel component is the nozzle, formed by converging and diverging sections that accelerate the air flow. A schematic of a supersonic wind tunnel set-up is shown in Figure 1.1.

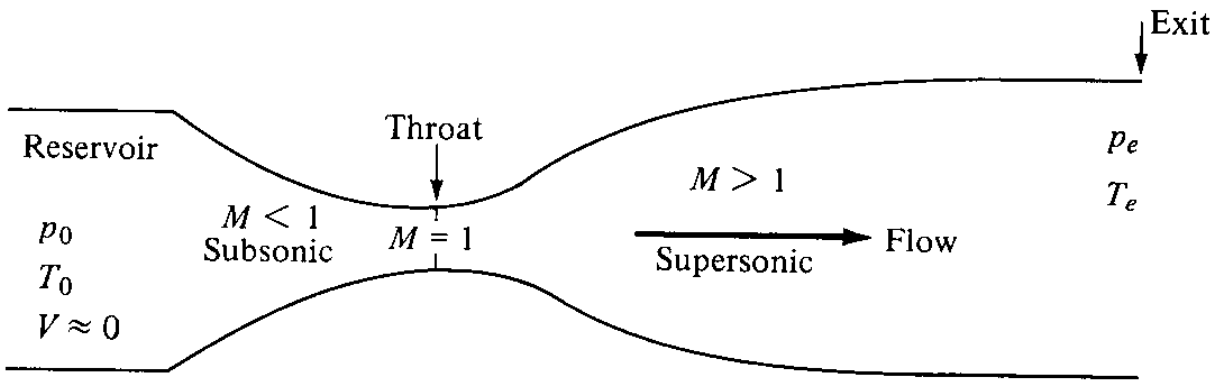

Figure 1.1: Schematic for supersonic nozzle (reprinted from Anderson [1], page 128).

There are many considerations that must be made when designing the shape of a wind tunnel nozzle. For example, turning sections with a small radius of curvature can cause flow separation. Additionally, the wall shape of the nozzle must be designed such that there are no undesired shock-waves inside the nozzle. These considerations, along with others described later, make it no small task to design a supersonic wind tunnel nozzle.

1.2 Background

The most basic explanation of a wind tunnel is the acceleration of a gas, such as air, from a speed slower than the speed of sound, or subsonic, to one greater than the speed of sound, also known as supersonic. A key aspect of supersonic flow is the formation of shockwaves, which are thin regions in the flow across which the properties can change drastically [2]. For reliable wind tunnel testing data, it is imperative to deliver straight, shock-free flow to the test section for the test article. This uniformity is achieved by carefully designing the shape of the nozzle wall.

The method of characteristics (MOC) has long been utilized to solve the gas dynamics equation, which governs flow in a nozzle. Ludwig Prandtl and Adolf Busemann devised the graphical approach to characterizing supersonic irrotational flow in a nozzle in 1929 [3]. This work has been built upon extensively, and is still in use today for nozzle design. Relevant works are summarized herein.

Before the MOC was widely used, methods such as that described by Crown [4] were utilized. Crown outlined in 1950 a method of nozzle design by first assuming a given velocity distribution along the axisymmetric nozzles centerline. Nozzle ordinates and velocity were expressed as truncated infinite series, which converge for low Mach number cases. This method is similar to converting source flow into a uniform stream at the exit, but instead finds the velocity distribution at the exit. The techniques described in Crown's paper were expanded upon and summarized by Yu [5]. He touched on the design of wind tunnel facilities, including heaters, thermal mixers, and fixed or adjustable diffusers. Additionally, Yu covered the characterization of wind tunnel parameters, such as run time and controls.

At the height of innovation in wind tunnels, Sivells [6] authored a comprehensive guide for nozzle design by the MOC. This included techniques for approximating the boundary layer (BL) to apply viscous corrections to the MOC, known as the MOC/BL method. McCabe [7], Prince [8], Wolf [9], and Hartfield [10] also produced important contributions to nozzle design using the MOC, such as summaries of available methods and details about implementation of the theory.

Wind tunnel facilities with flexible-walled supersonic nozzles have the advantage of providing

a range of test conditions for a constant-area test section. These facilities often have a discontinuity in curvature at the inflection point, resulting in imperfections in the flow. Early work by Evvard [11] aimed to fix this discontinuity by developing auxiliary conditions to assure continuous wall curvature. These conditions include:

- The geometric inflection point on the nozzle must be upstream of the final characteristic intersection with the tunnel centerline.
- The cancellation Mach line must be tangent to the test-section at the exit lip.

Evvard noted that this method will not produce minimum-length nozzles. This method was evaluated and validated by Yen [12]. He found that the method proposed by Evvard provided a perfectly straight, uniform test rhombus at the exit of a variable Mach number, constant length and diameter nozzle.

In addition to wind tunnels, nozzles are also critical for rocket flight. Fuel is combusted to create favorable stagnation conditions in a combustion chamber, then accelerated in a nozzle to provide thrust to the vehicle. Rocket nozzle design centers around maximizing the thrust produced coupled with reducing the weight and length of the nozzle. Ostlund [13] documented the different types of rocket nozzles, including ideal nozzles, which are also widely used for wind-tunnels. His paper studied flow separation induced by viscous forces and the resulting side-loads on the rocket nozzle wall. Ostlund stated that flow separation occurs in nozzles with small radii of curvature in the expansion region. Goeing [14] presented a method of optimizing rocket nozzle performance using the MOC. This was determined to require a constant change of the area ratio of the throat. Maximizing thrust, minimizing length, and effects of geometry changes on the nozzle were investigated. Young [15] presented an axisymmetric derivation that included finite-rate chemical kinetics for rocket nozzle design.

Rocket nozzles usually have downstream throat contours with much smaller radii of curvature when compared to wind tunnels nozzles. In the past, one rule-of thumb was that the radius of curvature in the downstream throat contour cannot be less than the throat radius. Kliegal [16]

postulated that this limitation was caused by an inappropriate choice of cylindrical coordinate system. Kliegal derived transonic perturbation equations in toroidal coordinates, and experimental results confirmed that this coordinate transformation more adequately described transonic flow in the small radius of curvature regime. This phenomena was also studied by Hopkins [17], who found that the radius of curvature could get as small as one quarter of the throat radius. Additionally, Hopkins concluded that the settling chamber contour does not affect the flow in the sonic region, as long as its radius of curvature is greater than the throat radius.

In addition to rockets, nozzles are used to expand the combustion products of air-breathing engines. Modern aircraft designs may require nozzle shapes deviating from the traditional designs. Two-dimensional MOC is limited by axisymmetric or planar nozzle design. This can be extended to three dimensional flow for bodies of revolution, which is covered by Rakich [18]. For non-conventional nozzles, Jegede [19] presented a technique of superimposing two-dimensional characteristics onto a three-dimensional non-axisymmetric nozzle geometry. Jegede illustrated an application of this method in the exhaust flow in stealth aircraft.

As the aerospace field has shifted its focus to hypersonic flight, new challenges have arisen regarding hypersonic wind tunnels. Benton [20] found limitations of the MOC in the hypersonic regime. He explored compression waves that appear in hypersonic nozzles originating from the inflection point where the nozzle transitions from concave to convex. Benton found that while all nozzles show evidence of these compression waves, their effects in the downstream flow are largely negligible until Mach 8. Candler [21] further explored this irregularity by examining the effects of vibrational nonequilibrium on axisymmetric hypersonic nozzles. He performed a number of CFD simulations on nozzles designed by the MOC/BL method, with vibrational energy assumed to be variable and frozen. There were two significant results:

- The assumption of vibrational equilibrium breaks down for hypersonic nozzles, where the vibrational temperature freezes soon after the throat.
- Characteristics in thick hypersonic boundary layers do not adhere to the assumption in the method of characteristics that characteristics do not penetrate the boundary layer. This pen-

etration causes the underprediction of the length of nozzle required to expand the flow to the design Mach number.

These two results were found to offset each other, which results in a reasonably accurate nozzle contour. Candler also found that increasing the stagnation pressure by a factor of five or extending the throat resulted in delayed vibrational freezing.

These limitations in the hypersonic regime led to the development of an advanced method of nozzle design, called the design-by-analysis. Korte ([22], [23], [24]) demonstrated this method by utilizing a parabolized Navier-Stokes CFD solver coupled with an optimization algorithm to produce hypersonic nozzles with minimized flow perturbations and angularity at the design test conditions. The design-by-analysis method was also briefly described by Shope [25]. This method requires an initial nozzle contour, which is usually generated by the MOC/BL method. Chan [26] followed the methods of Korte([22], [23], [24]) and proved that CFD optimization resulted in less property fluctuations at the nozzle exit, even for nozzles at Mach 4, which is well below the hypersonic classification.

Although a commercial nozzle design code does not currently exist, Sivells [27] developed a code for distribution, called CONTUR, for nozzle design by the MOC, which was then summarized by Shope [25]. Sivells' method requires the centerline Mach number distribution to be pre-defined. This code has been used to successfully design and create nozzles, which is illustrated by Adams [28]. Other recent work with nozzle design includes work by Yoshio [29], who used Prandtl-Meyer expansion waves to determine the conditions induced by the initial expansion region.

Several textbooks, such as Anderson's *Modern Compressible Flow* [30], cover a superficial approach to the MOC. This text offers an introduction to the method, but does not contain details on nozzle design. In contrast, *Gas Dynamics* by Zucrow and Hoffman ([31],[32]) comprehensively details the MOC for the design of supersonic nozzles. They utilized a unit approach by numerical integration that eliminated the need for Prandtl-Meyer expansion theory, which is limited by the assumption of a sharp turning region. This numerical method permits greater flexibility when

defining the geometry of the nozzle. The textbooks cover both planar and axisymmetric nozzles, and was utilized heavily for the work of this thesis.

Works that directly influenced the development of this code are depicted in Figure 1.2. Additionally, Figure 1.3 presents a summary of the background research performed above.

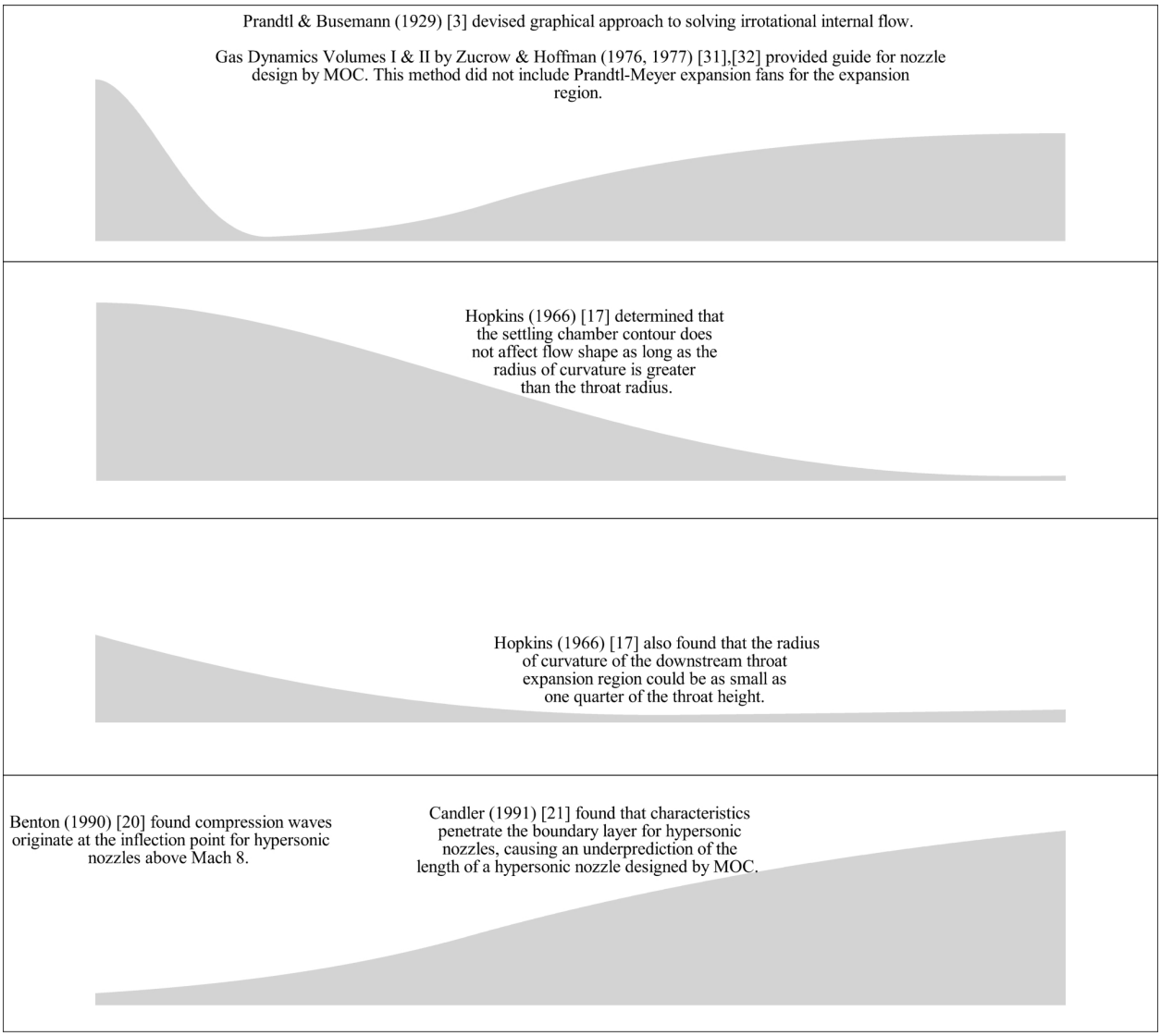

Figure 1.2: Resources that directly influenced MOC code development.

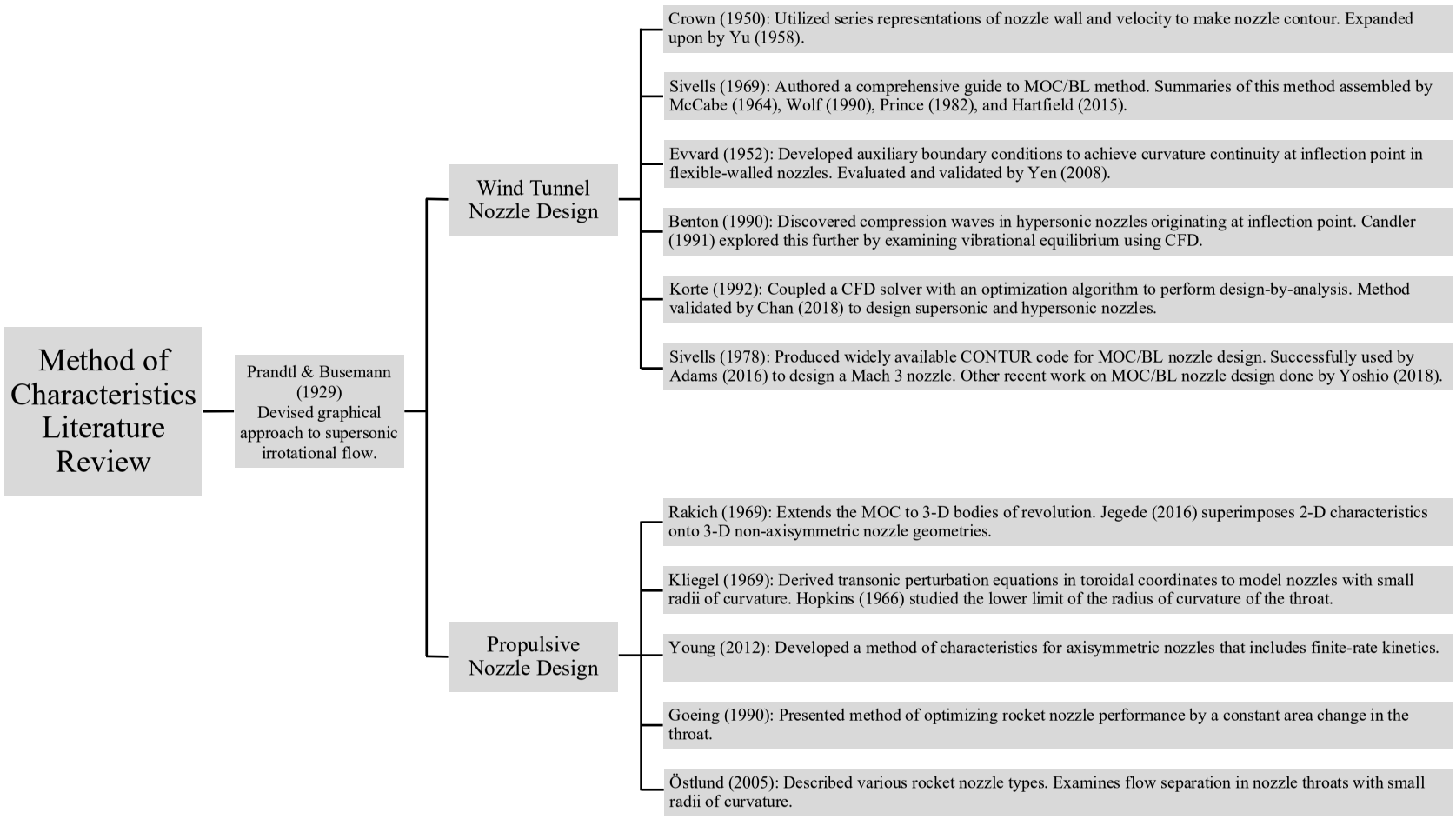

Figure 1.3: Summary of background.

1.3 Research Objectives

The objective of this work is to develop a MOC code for designing state-of-the-art supersonic nozzles at the Texas A&M University National Aerothermochemistry & Hypersonics Laboratory. This code permits the user to input various geometry parameters to achieve a design that meets the desired test conditions.

Currently, two nozzles at the National Aerothermochemistry & Hypersonics Laboratory were designed using a MOC code written in Fortran by Dr. Bowersox, a planar code which allows the user to input both the exit Mach number and initial wall turning angle downstream of the initial radius of curvature. This code is limited to planar flows and the initial wall radius is limited, especially at hypersonic Mach numbers. A more general code available only allows the user to input the number of characteristic reflections used to design the nozzle, necessitating a guess-and-check method to achieve the design Mach number. The present MOC code eliminates the limitations associated with both of these codes by allowing specification of the design Mach number as an input, eliminating time consuming design iterations, and permitting greater freedom over the geometry of the nozzle. In summary, the new code significantly expands the tools available at the National Aerothermochemistry & Hypersonics Laboratory for future experimental needs.

2. DERIVATION OF GOVERNING EQUATIONS

To design a supersonic nozzle, an equation satisfying the design conditions of straight, shock-free flow must first be developed. The gas dynamics equation was derived in the following sections following the method outlined in [31], followed by application of the MOC to the derived equation.

2.1 Governing Equation

Deriving the gas dynamics equation began with the conservation of mass equation expressed with the substantial derivative.

$$\frac{D\rho}{Dt} + \rho\nabla \cdot \overrightarrow{V} = 0 \tag{2.1}$$

The speed of sound was expressed as $a^2 = (\frac{\partial p}{\partial \rho})_s$. Assuming the flow was isentropic and that time derivatives were determined, this was expressed in terms of the substantial derivative.

$$\frac{Dp}{Dt} - a^2\frac{D\rho}{Dt} = 0 \tag{2.2}$$

This form of the speed of sound equation was substituted into equation 2.1 and, after assuming steady flow, was expressed in equation 2.3.

$$\left(\overrightarrow{V} \cdot \nabla\right) p + a^2\rho\nabla \cdot \overrightarrow{V} = 0 \tag{2.3}$$

Next the inviscid, adiabatic, compressible momentum equation with no body forces or external work was utilized to apply the irrotational flow condition.

$$\rho\frac{D\overrightarrow{V}}{Dt} + \nabla p = 0 \tag{2.4}$$

Assuming steady flow and employing vector identities, as well as the condition for irrotational

flow ($\nabla \times \overrightarrow{V} = 0$) lead to Euler's equation for steady, irrotational flow (2.5).

$$\nabla p + \rho \nabla \left(\frac{V^2}{2} \right) = 0 \tag{2.5}$$

The scalar product of equation 2.5 was taken and the result was combined with equation 2.3 to eliminate the ∇p term, leading to the gas dynamic equation (2.6).

$$\rho \left(\overrightarrow{V} \cdot \nabla \right) \left(\frac{V^2}{2} \right) - a^2 \rho \nabla \cdot \overrightarrow{V} = 0 \tag{2.6}$$

The gas dynamic equation was expanded into Cartesian coordinates and simplified to two dimensions, defining the action of planar and axisymmetric, compressible, adiabatic, irrotational flow [31]($\delta = 1$ for axisymmetric, $\delta = 0$ for planar). This equation is a non-linear Partial Differential Equation (PDE). The resulting equation, along with the irrotational condition, formed the governing equations for irrotational, compressible, inviscid flow in a nozzle.

$$\begin{aligned} (u^2 - a^2)\frac{\mathrm{d}u}{\mathrm{d}x} + (v^2 - a^2)\frac{\mathrm{d}v}{\mathrm{d}y} + 2uv\frac{\mathrm{d}u}{\mathrm{d}y} - \frac{\delta a^2 v}{y} &= 0 \\ \frac{\mathrm{d}v}{\mathrm{d}x} - \frac{\mathrm{d}u}{\mathrm{d}y} &= 0 \end{aligned} \tag{2.7}$$

2.2 Characteristic Equation

The classification of PDE that the gas dynamics equation takes depends on the discriminant of the equation. The discriminant was taken from the coefficients of the highest-order differential terms, shown in Equation 2.8.

$$\underbrace{(u^2 - a^2)}_{\text{A}} \frac{\mathrm{d}u}{\mathrm{d}x} + \underbrace{(2uv)}_{\text{B}} \frac{\mathrm{d}u}{\mathrm{d}y} + \underbrace{(v^2 - a^2)}_{\text{C}} \frac{\mathrm{d}v}{\mathrm{d}y} \tag{2.8}$$

The resulting expression was reduced to the condition that $M^2 - 1$ must be either less than zero, equal to zero, or greater than zero. If the discriminant is less than zero, then the PDE is elliptic and the flow is subsonic, with imaginary characteristics. If it is equal to unity, then the equation is

parabolic and the flow is exactly sonic, with one real characteristic passing through each point in the flowfield. Lastly, a discriminant greater than zero indicates that the equation is hyperbolic, and the subsequent flow is supersonic [30], with two real characteristics passing through each point in the flowfield. Hyperbolic equations can be solved by direct marching techniques starting from an initial value line. The most accurate of these techniques for quasi-linear PDE's is the method of characteristics [31]. This method states that in any hyperbolic PDE, there are a set of characteristics along which properties will propagate downstream. These characteristics are curves along which the governing PDE can be reduced to a set of ordinary differential equations. Properties along these characteristics must be continuous, but the derivatives of the property may be discontinuous. The MOC was utilized to reduce the system of hyperbolic PDE's shown in equation 2.7 to a system of Ordinary Differential Equations (ODE's) that were solved with numerical integration along the characteristic lines.

The two equations were multiplied by the unknown parameters σ_1 and σ_2, respectively, and added together. The coefficients of the partial derivatives of u and v were then factored out and grouped together.

$$\sigma_1 \left(u^2 - a^2\right) \left[\frac{\sigma_1(2uv) + \sigma_2}{\sigma_1(u^2 - a^2)} u_y\right] + (-\sigma_2) \left[v_x + \frac{\sigma_1(v^2 - a^2)}{-\sigma_2} v_y\right] - \sigma_1 \frac{\delta a^2 v}{y} = 0 \tag{2.9}$$

If u(x,y) and v(x,y) were assumed to be continuous, then the following relations were true.

$$\begin{aligned} \frac{\mathrm{d}u}{\mathrm{d}x} &= u_x + \lambda u_y \\ \frac{\mathrm{d}v}{\mathrm{d}x} &= v_x + \lambda v_y \end{aligned} \tag{2.10}$$

Comparing equation 2.10 to equation 2.9, there were two values for λ.

$$\begin{aligned} \lambda &= \frac{\sigma_1(2uv) + \sigma_2}{\sigma_1(u^2 - a^2)} \\ \lambda &= \frac{\sigma_1(v^2 - a^2)}{-\sigma_2} \end{aligned} \tag{2.11}$$

Equation 2.11 was rearranged to solve for the coefficients σ_1 and σ_2. The solution of these coefficients required that the determinant of their variable coefficients must equal zero.

$$\left(u^2 - a^2\right)\lambda^2 - 2uv\lambda + \left(v^2 - a^2\right) = 0 \tag{2.12}$$

The quadratic formula, followed by variable reduction, were employed to find an expression for λ. This relation specified two curves in the x-y plane that are real when the Mach number is greater than one.

$$\lambda_{\pm} = \left(\frac{\mathrm{d}y}{\mathrm{d}x}\right)_{\pm} = \frac{uv \pm a^2\sqrt{M^2 - 1}}{u^2 - a^2} \tag{2.13}$$

Trigonometric relations for the flow properties along a streamline were derived from Figure 2.1 and then employed to simplify equation 2.13 into a form more suitable for MOC analysis.

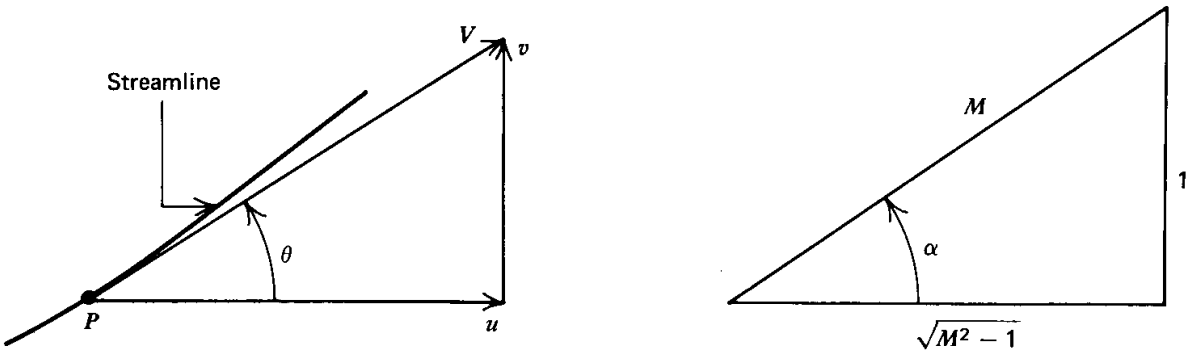

Figure 2.1: Streamline geometries for deriving alternate form of characteristic equation (reprinted from Zucrow & Hoffman [31], page 594).

$$\lambda_{\pm} = \left(\frac{\mathrm{d}y}{\mathrm{d}x}\right)_{\pm} = \tan\left(\theta \pm \alpha\right) \tag{2.14}$$

Equation 2.14 governs the shape of the left and right-running characteristics that stem from a streamline in supersonic flow, shown in Figure 2.2. It is along these curves that flow information is propagated downstream.

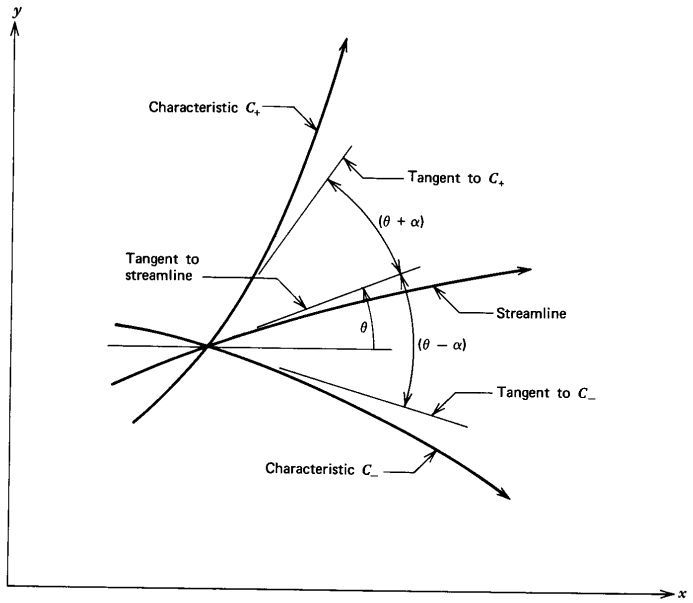

Figure 2.2: Left and right-running characteristics stemming from streamline (reprinted from Zucrow & Hoffman [31], page 595).

2.3 Compatibility Equation

An equation relating flow variables must be found to describe the flow properties along the characteristic lines. This equation is the the compatibility equation. First, equations 2.10 and 2.11 were substituted into equation 2.9 and simplified.

$$\sigma_1 \left(u^2 - a^2\right) du - \sigma_2 dv - \left(\frac{\sigma_1 \delta a^2 v}{y}\right) dx = 0 \tag{2.15}$$

Equation 2.15 governs the relationship between u and v along a characteristic. It was rearranged to eliminate σ_1 and σ_2.

$$\begin{aligned} \sigma_2 &= \sigma_1 \left[\left(u^2 - a^2\right) \lambda - 2uv\right] \\ \sigma_2 &= -\sigma_1 \frac{v^2 - a^2}{\lambda} \end{aligned} \tag{2.16}$$

The expressions in equation 2.16 are dependent on each other, and therefore either one may be substituted into equation 2.15. The resulting expression is the compatibility equation used for

implementing the MOC. This ODE relates the flow properties u and v along a characteristic.

$$\left(u^2 - a^2\right) du_{\pm} + \left[2uv - (u^2 - a^2)\lambda_{\pm}\right] dv_{\pm} - \left(\frac{\delta a^2 v}{y}\right) dx_{\pm} = 0 \tag{2.17}$$

3. NUMERICAL IMPLEMENTATION

3.1 Parameter Inputs & Settling Chamber

The region of a nozzle joining the converging and diverging sections is commonly known as the throat. The throat contains the smallest cross-sectional area of the nozzle, and is where the flow is exactly sonic. The throat can be defined by a variety of different shapes, such as a polynomial or a hyperbola. A circular throat region was found sufficient for this code. The geometric design parameters include the throat height, the radius of curvature of the initial expansion contour, and the turning angle of the circular region, shown in Figure 3.1. Additionally, the nozzle must be defined as axisymmetric or planar.

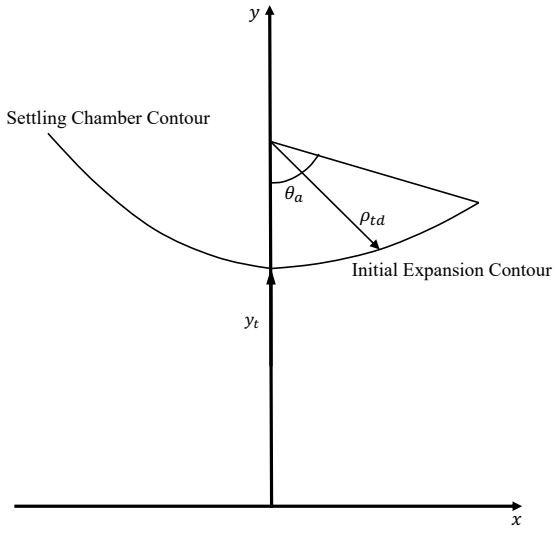

Figure 3.1: Geometric parameters in throat of supersonic nozzle.

The settling chamber is an area immediately upstream of a nozzle throat that stagnates the incoming flow by rapidly expanding it from a small area to a larger area. The flow conditions in the settling chamber must also be defined, including stagnation temperature and pressure, the

gas constant and ratio of specific heats of the gas, and the design Mach number. A fourth-order polynomial was chosen to define the settling chamber contour. The most important condition for settling chamber design was ensuring continuity at the junction of the settling chamber and expansion contour to the second derivative. Not upholding this condition could result in undesired Mach waves generated at this point in the throat. The user inputs the design length and height of the settling chamber entrance, denoted as L and H. Equation 3.1 lists the fourth-order polynomial and the associated boundary conditions for designing the settling chamber.

$$\begin{aligned} y(x) &= Ax^4 + Bx^3 + Cx^2 + Dx + E \\ y(0) &= y_{throat} \\ y'(x) &= 0 \\ y''(x) &= \frac{\mathrm{d}^2 y_{throat}}{\mathrm{d}x^2} \\ y(-L) &= H \\ y'(-L) &= 0 \end{aligned} \tag{3.1}$$

3.2 Sonic Line

The boundary of sonic flow in the throat, shaped like a parabola, is called the sonic line. Figure 3.2 demonstrates that the sonic line intersects the nozzle wall upstream of the minimum-area point, denoted by T. Calculation of the location and properties of the sonic line are covered in [32].

To initiate the MOC, a line must be used along which the Mach number is greater than one across the entire throat. The sonic line is therefore unsuitable for this application. A straight Mach line at an angle of $sin^{-1}(\frac{1}{M})$ from the horizontal was drawn from point T on the throat wall and extends into the region of supersonic flow. This initial value line was initialized to either a Mach number near one for a converging-diverging nozzle, or a Mach number greater than one for a diverging nozzle. This became the starting point for the MOC to propagate a solution downstream.

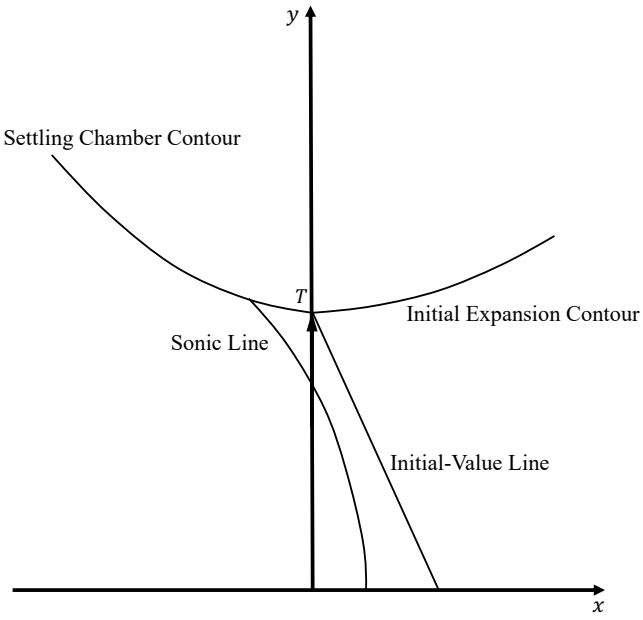

Figure 3.2: Sonic line and initial-value line in supersonic nozzle throat.

3.3 Modified Euler Predictor-Corrector Method

The compatibility equation provides a single equation relating flow properties u and v. To obtain two relationships for calculating these properties in the flow field, a network must be created with intersecting characteristics. At the intersection point, there is one relationship between u and v on each of the intersecting characteristics, and therefore there are two equations with two unknowns at the that location. Figure 3.3 demonstrates left and right-running characteristics intersecting at point 4, where a solution for flow variables was found. This method was easily modified for a wall or axis of symmetry point. For the wall, the left-running characteristic must intersect at the predefined wall location, and the flow must follow the curve of the wall, demonstrated in Figure 3.4. In a similar manner, an axis of symmetry point would have $y = v = 0$, and as such the characteristic and compatibility equations can be solved without a second intersecting characteristic, shown in Figure 3.5.

The characteristic equation and compatibility equation are nonlinear ordinary differential equa-

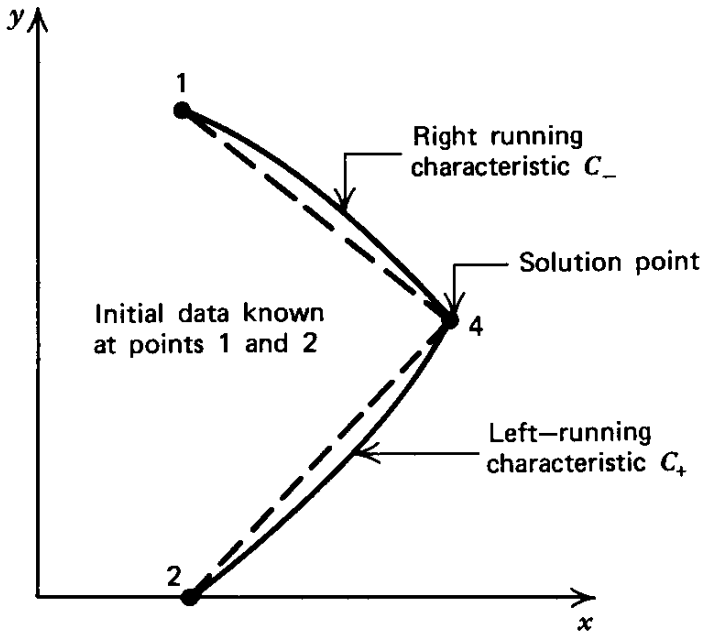

Figure 3.3: Finite difference network for applying the MOC for an interior point (reprinted from Zucrow & Hoffman [31], page 603).

tions. Their solutions are obtained by finite difference techniques, namely the modified Euler predictor-corrector method [31]. This is a second-order method for integrating ordinary differential equations. The corrector algorithm is based on the average property method, wherein the values of the coefficients of the differential equations are determined by averaging the values of the properties at the initial point and the solution point. The finite difference equations for steady, inviscid, isentropic nozzle flow are presented in equation 3.2, where $+$ or $-$ represent left-running C_+ or right-running C_-, respectively [31].

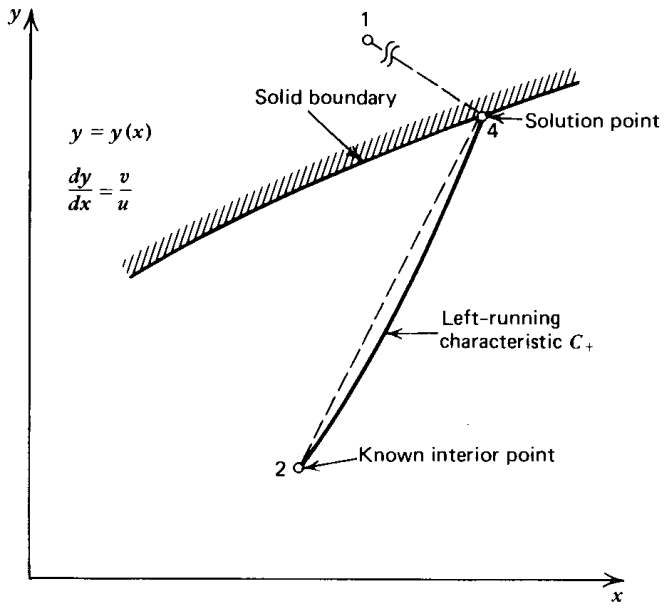

Figure 3.4: Boundary conditions for applying the MOC to a wall point (reprinted from Zucrow & Hoffman [32], page 125).

$$
\begin{aligned}
\Delta y_{\pm} &= \lambda_{\pm}\Delta x_{\pm} \\
Q_{\pm}\Delta u_{\pm} + R_{\pm}\Delta v_{\pm} - S_{\pm}\Delta x_{\pm} &= 0 \\
\lambda_{\pm} &= \tan(\theta \pm \alpha) \\
Q &= u^2 - a^2 \\
R &= 2uv - (u^2 - a^2)\lambda \\
S &= \delta\frac{a^2 v}{y}
\end{aligned}
\tag{3.2}
$$

The corrector algorithm was iterated by substituting the result of the corrector to the average property calculation, then applying the corrector again. This algorithm is applied until the desired convergence is met. Convergence criteria was defined according to [31], shown below. P represents flow variables, including x_4, y_4, u_4 and v_4. Recommended tolerance was $0.0001m$ for location and $0.1m/s$ for velocity components. The Euler predictor-corrector method converged rapidly, typically by the second or third application of the corrector.

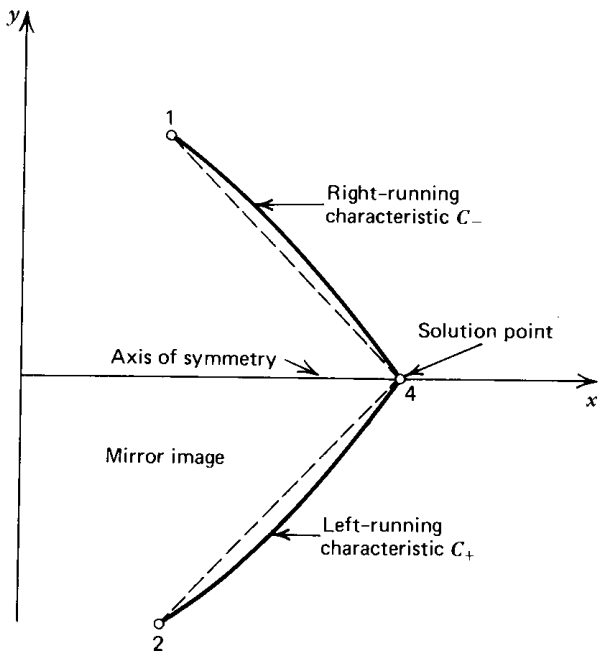

Figure 3.5: Boundary conditions for applying the MOC to an axis of symmetry point (reprinted from Zucrow & Hoffman [32], page 135).

$$\left|P^n - P^{n-1}\right| \leq \text{(specified tolerance)} \tag{3.3}$$

3.4 Nozzle Contour Design

Once the initial value line was established, the MOC solution was marched downstream, again using the modified Euler predictor-corrector method. The intersection of a left-running wave from the initial value line with the wall was found, and the flow properties at this point computed. This became the starting point for a right-running wave, which was propagated downstream until it intersected the axis of symmetry. A new left-running wave was taken from this new characteristic, and the process was repeated down the nozzle, illustrated in Figure 3.6.

This process was completed when the design Mach number is met on the tunnel centerline from a right-running characteristic. If this had not occurred when the throat was characterized, then the mass flow rate condition was imposed until the design Mach number was met. This principle,

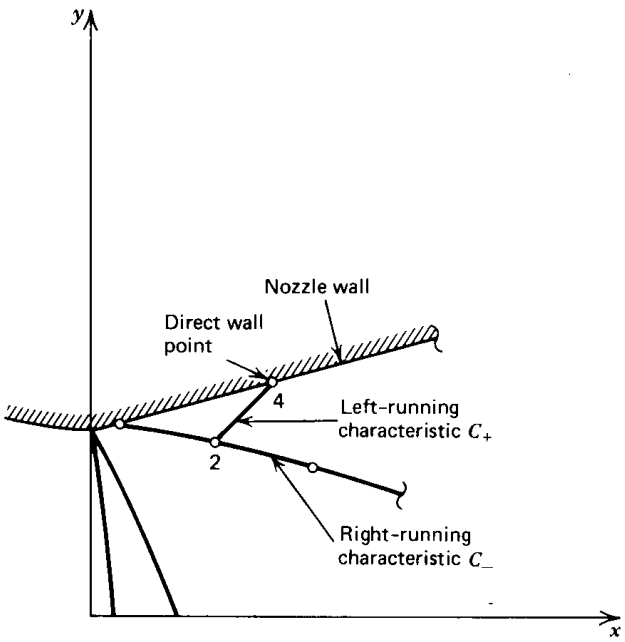

Figure 3.6: Illustration of MOC solution marching through nozzle throat (reprinted from Zucrow & Hoffman [32], page 148).

that mass is conserved, was useful for calculating the nozzle wall contour. Since the flow was choked at the throat, the mass flow rate across any characteristic in the nozzle must equal the mass flow rate through the throat. The mass flow rate was calculated by integrating $d\dot{m} = \rho V dA$ using Simpson's rule [32]. Left-running characteristics continued to be extended to make new right-running characteristics. The length of the right-running characteristics was constrained by the mass flow rate through them, thus extending the concave portion of the nozzle contour.

The flow was ready to be straightened when the design Mach number was met on the nozzle centerline from a right-running characteristic, depicted as point K on Figure 3.7. For the exit flow field to be parallel uniform flow, all of the characteristics in region R must be straight lines at the Mach angle $\sin^{-1}\left(\frac{1}{M_D}\right)$ [32], denoted α_D. This Mach line was extended until the mass flow rate across the line was equal to the mass flow rate through the throat. Point F was the exit lip point of the nozzle.

The turning, or convex, contour was determined by performing the interior-point process, utilizing points on the line I-K and line K-F in Figure 3.8. Right-running characteristics were calcu-

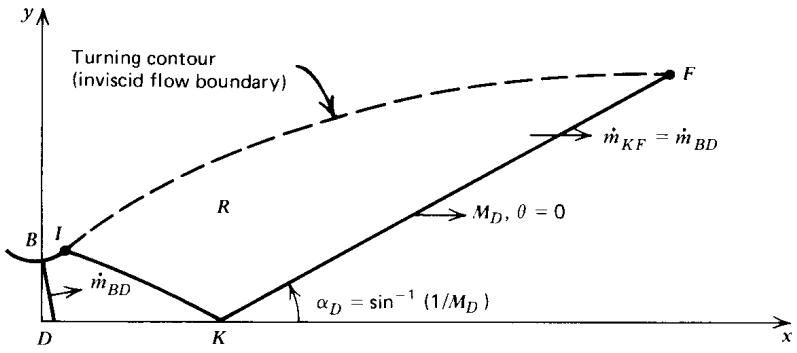

Figure 3.7: Turning region schematic (reprinted from Zucrow & Hoffman [32], page 161).

lated towards the nozzle wall, and the mass flow rate condition was used to terminate the characteristics at the wall. The result completely defines the nozzle contour for the design test conditions, providing straight, irrotational flow to the test section.

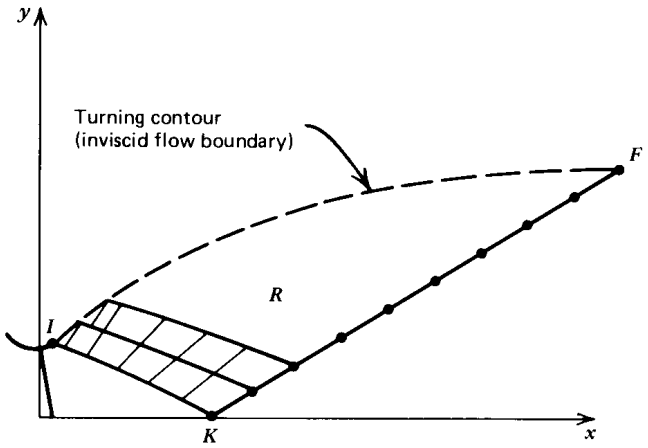

Figure 3.8: Turning region unit process (reprinted from Zucrow & Hoffman [32], page 163).

4. CFD VALIDATION

4.1 Simulation Software

The nozzle designs were validated using US3D version 1.1.8. US3D is a 3-dimensional computational fluid dynamics (CFD) code for the simulation of compressible and reacting flows [33]. The US3D code is a next-generation version of the NASA data-parallel line-relaxation (DPLR) structured code. US3D employs many of the same numerical methods as the NASA DPLR code, but permits the use of unstructured grids. It further expands the capabilities of the NASA code, including high-order, low-dissipation numerical flux methods, advanced turbulence models and dynamic grid motion. This solver was chosen due to prior experience with the software.

4.2 Meshing & Simulation Parameters

Once a nozzle contour was designed, the code outputted a text file with columns of x, y, z data, where the z values are all zero. This text file was uploaded to SolidWorks 2018 for conversion to a .iges file. This file was then uploaded into Pointwise V18.3 to produce the structured mesh.

The settling chamber was extended a small amount in each simulation to aid meshing. In a similar manner, the exit was extended a small amount to aid in post-processing the simulation.

Each converging-diverging nozzle simulation was initialized with an inviscid freestream flow field, subsonic in the settling chamber and supersonic in the expansion region. Similarly, the diverging nozzles were initialized with an inviscid supersonic freestream flow field. The simulation utilized an implicit DPLR time integration with four subiterations. This scheme was chosen for its quick convergence and robust nature for steady state problems. Simulations were performed with second order inviscid fluxes in space by modified Steger-Warming flux-vector splitting, with second order MUSCL flux extrapolation. This was deemed appropriate because there was not a boundary layer or small-scale structures present in the simulation. Perfect gas conditions were assumed, neglecting chemical and vibrational effects. This was considered a reasonable assumption for engineering-level designs.

The inlet was assigned a characteristic subsonic inflow condition, defined by stagnation pressure and temperature. The outflow boundary condition was defined as a supersonic outflow, which uses an extrapolation of the upstream conditions. An isothermal wall boundary condition was imposed on the nozzle contour, where the temperature was assigned room temperature. The axis of symmetry at the tunnel centerline was assigned a symmetry face condition. Simulation boundary conditions are illustrated in Figure 4.1. Although inviscid nozzles can be simulated in two-dimensions, this solver does not have that capability. However, US3D offers a periodic boundary condition for axisymmetric or planar boundaries. For axisymmetric nozzles, the 2-D nozzle contour was rotated $\pm 0.5^{\circ}$ along the x-axis to create a small wedge. Planar nozzles, in a similar fashion, were extruded a small amount in the z-direction to create a small 3-D prism. These methods are illustrated in Figure 4.2.

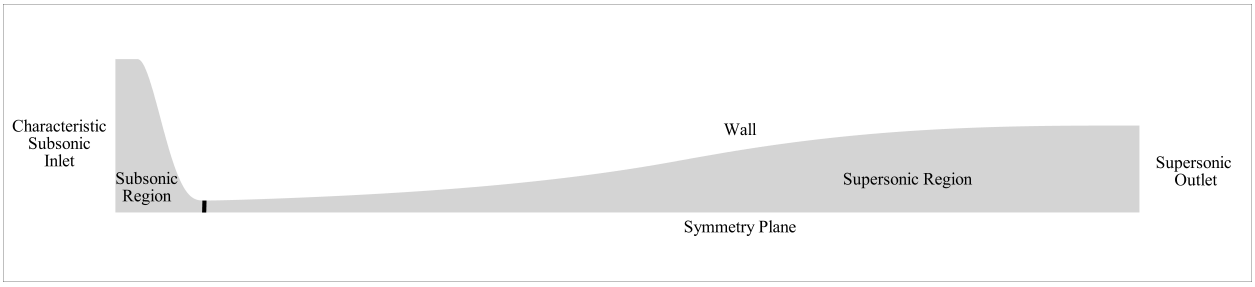

Figure 4.1: Two-dimensional boundary conditions for simulation.

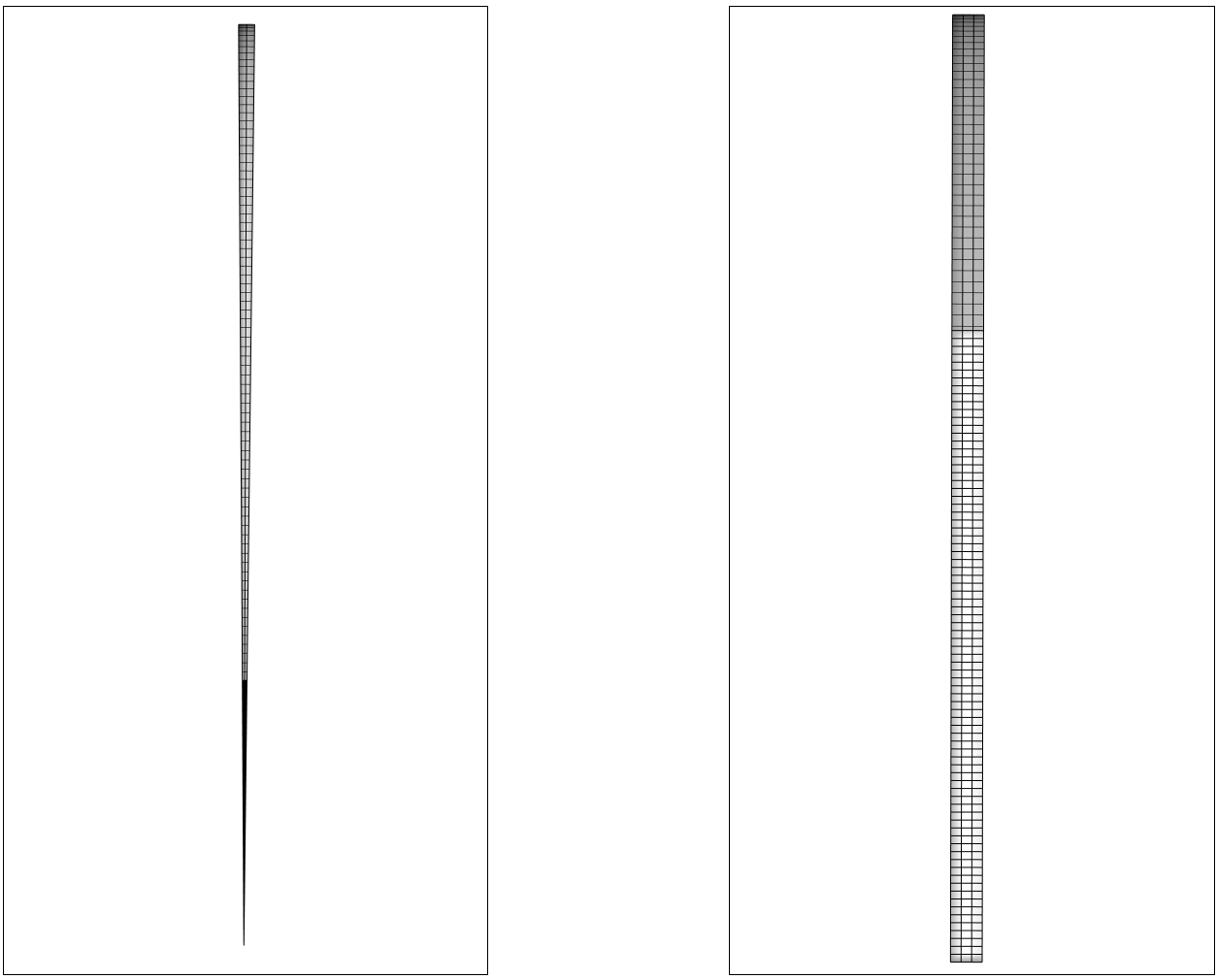

(a) Axisymmetric grid slice.

(b) Planar nozzle extrusion.

Figure 4.2: Method of meshing 3-D axisymmetric and planar nozzles.

4.3 Results

The MOC code was successful when a nozzle contour makes uniform, irrotational flow with the design Mach number at the exit plane. Flow in an aerodynamic testing environment is considered uniform if the deviations of flow properties are within 0.25% of the mean [34]. The formula to calculate the deviation of each property was presented in equation 4.1. The experimental value was the local property value at each point along the mesh, and the mean was calculated as the average of all data points along the exit plane.

$$\%Deviation = \frac{|Experimental - Mean|}{Mean} \times 100 \tag{4.1}$$

4.3.1 Grid Independence

A grid independence study was conducted to ensure that the solutions would not be affected by the grid. In order for a solution to be grid independent, the solution must not change with mesh size. Three grids were generated, consisting of coarse, medium, and fine sizes. The coarse grid consisted of 32,250 cells on a 2-D plane. The amount of cells in the coarse mesh was increased by five and fifteen to create the medium and fine meshes, respectively. The medium grid contained 170,730 cells, and the fine grid had 498,000 cells. These meshes were extruded to a wedge and simulated as axisymmetric. A comparison of the solutions determined that the medium grid provided grid independence because variation in solution between the medium and fine meshes was negligible. The variation of exit-plane Mach number and temperature between the three meshes is illustrated in Figures 4.3 and 4.4. The solution for the medium grid, Mach 6 case is presented in Figure 4.6. This grid density was utilized for all results presented herein.

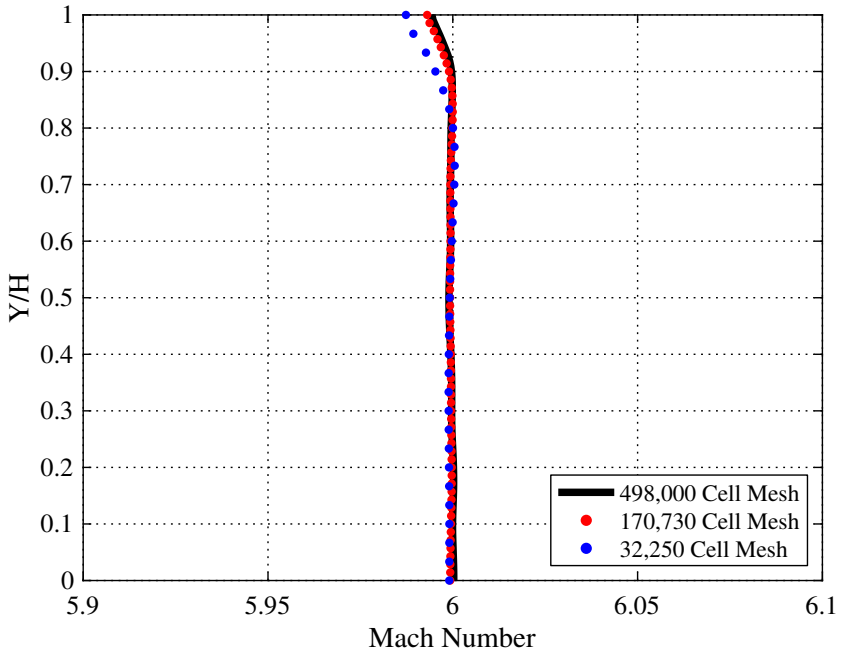

Figure 4.3: Mach number variation from grid independence study.

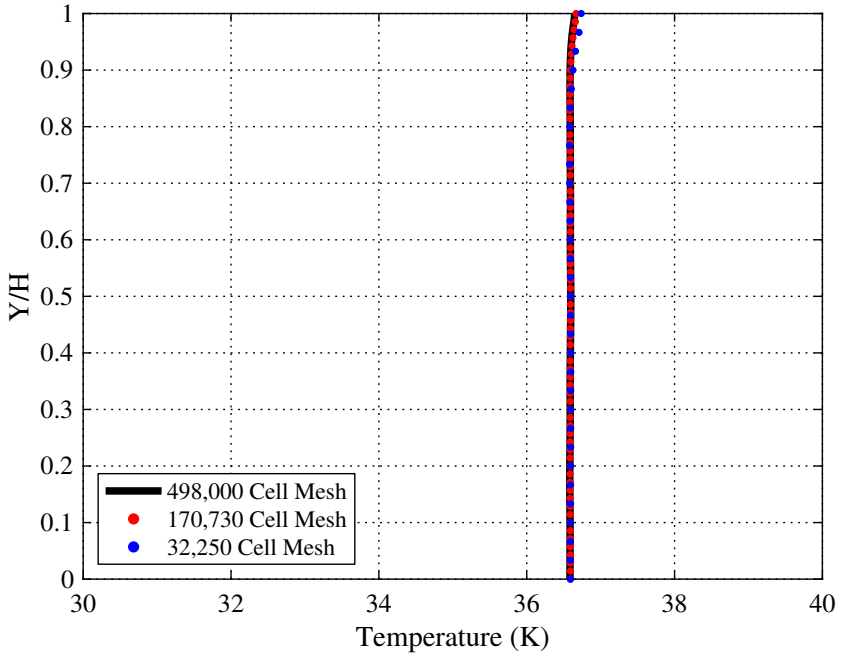

Figure 4.4: Temperature variation from grid independence study.

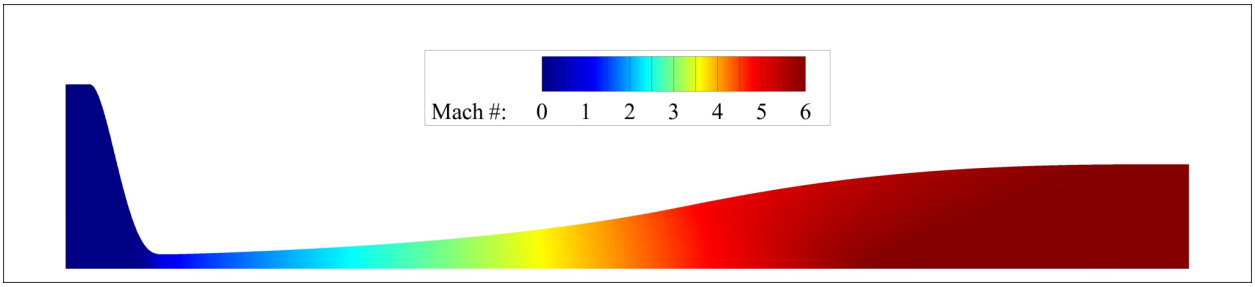

Figure 4.5: Mach 6 nozzle solution from medium mesh simulated in grid independence study.

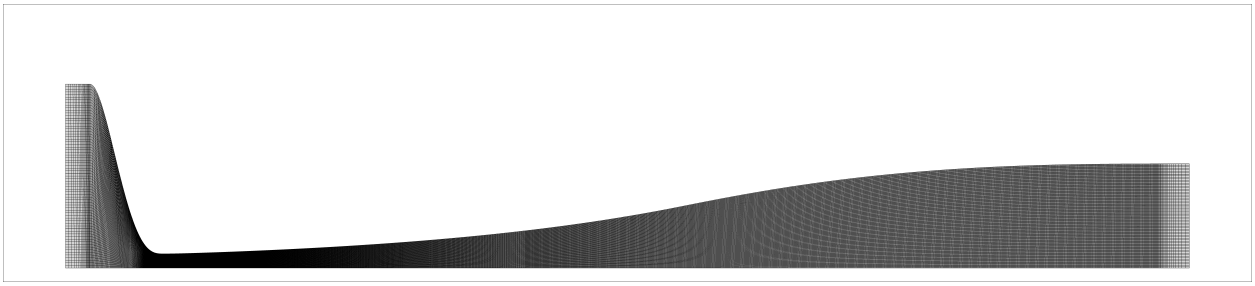

Figure 4.6: Mach 6 nozzle medium mesh from grid independence study.

4.3.2 Initial Throat Mach Number Sensitivity

When designing a converging-diverging nozzle, an initial value line near Mach 1 was drawn in the throat. Previous nozzles were designed with an initial value line of Mach 1.03 and produced successful simulations. A sensitivity study was performed on the initial Mach number to determine the effects of of this variation on the solution. The inlet Mach number was varied from 1.03 down to 1.005 for this study.

Each contour was simulated in US3D and the property variation of various parameters at the exit plane is presented in Figure 4.7. The results indicate that using Mach 1.03 as the initial-value line produced the least flow variation at the nozzle exit. Additionally, the solution time was reduced as the Mach number was increased. Mach 1.03 was used for all validation cases presented.

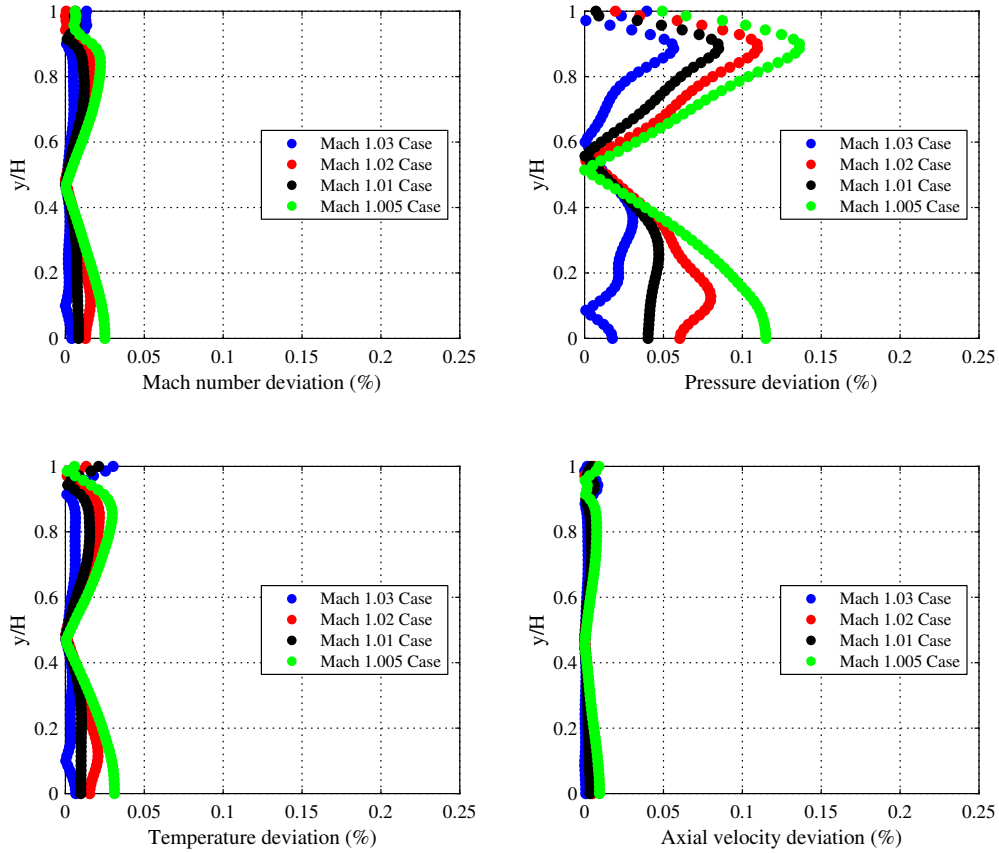

Figure 4.7: Property variation from initial throat Mach number sensitivity study.

4.3.3 Axisymmetric Mach 9 Converging-Diverging Nozzle

An axisymmetric Mach 9 converging-diverging nozzle was first generated. Figure 4.8 shows a full view of the Mach 9 nozzle. For flow uniformity at the exit plane, there must not be transverse velocity components after the characteristic cancellation. Figure 4.9 confirms the absence of transverse velocity in this region, and Figure 4.10 shows Mach 9 flow at the exit plane. Variation in the key flow parameters is presented in Figure 4.11. Deviations in the core-flow region are within acceptable tolerances defined above. The flow in the throat, presented in Figure 4.12, expands smoothly from subsonic to supersonic with the expected parabola-shaped sonic line. The X and Y density gradients are presented in Figures 4.13 and 4.14.

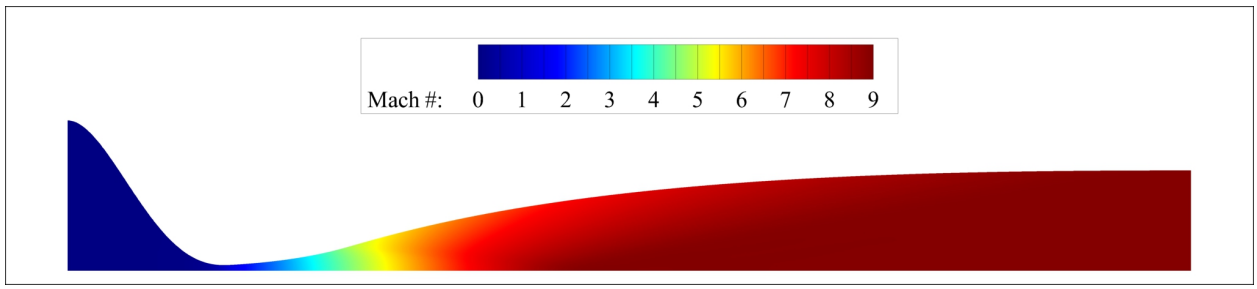

Figure 4.8: Axisymmetric Mach 9 nozzle full-view.

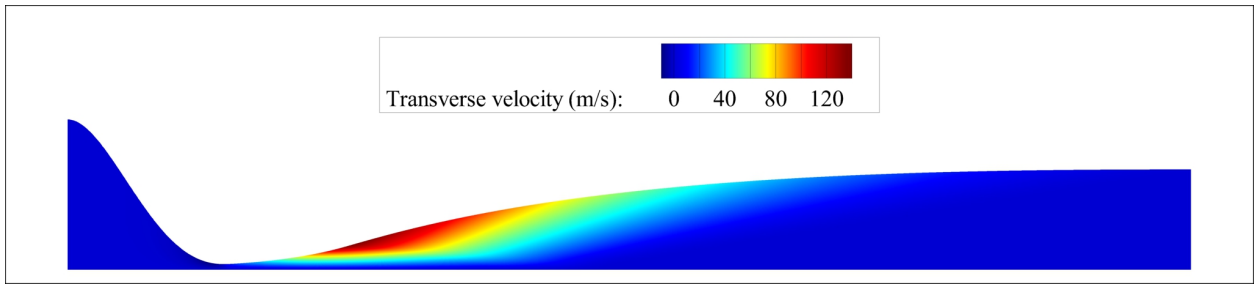

Figure 4.9: Axisymmetric Mach 9 nozzle transverse velocity.

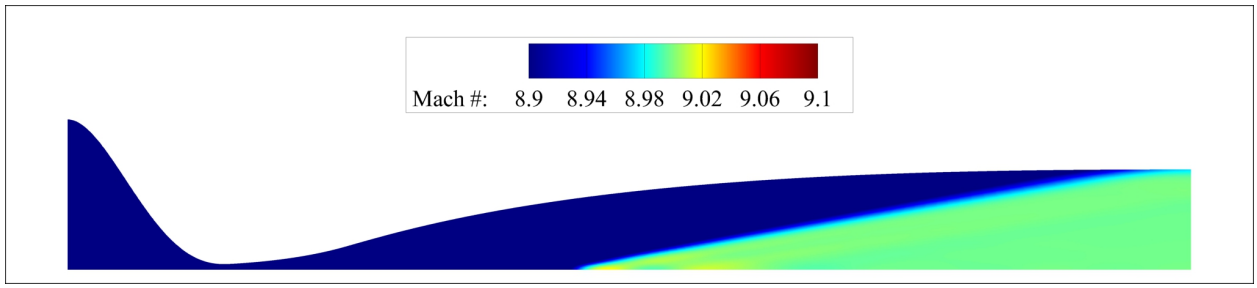

Figure 4.10: Axisymmetric Mach 9 nozzle exit Mach line.

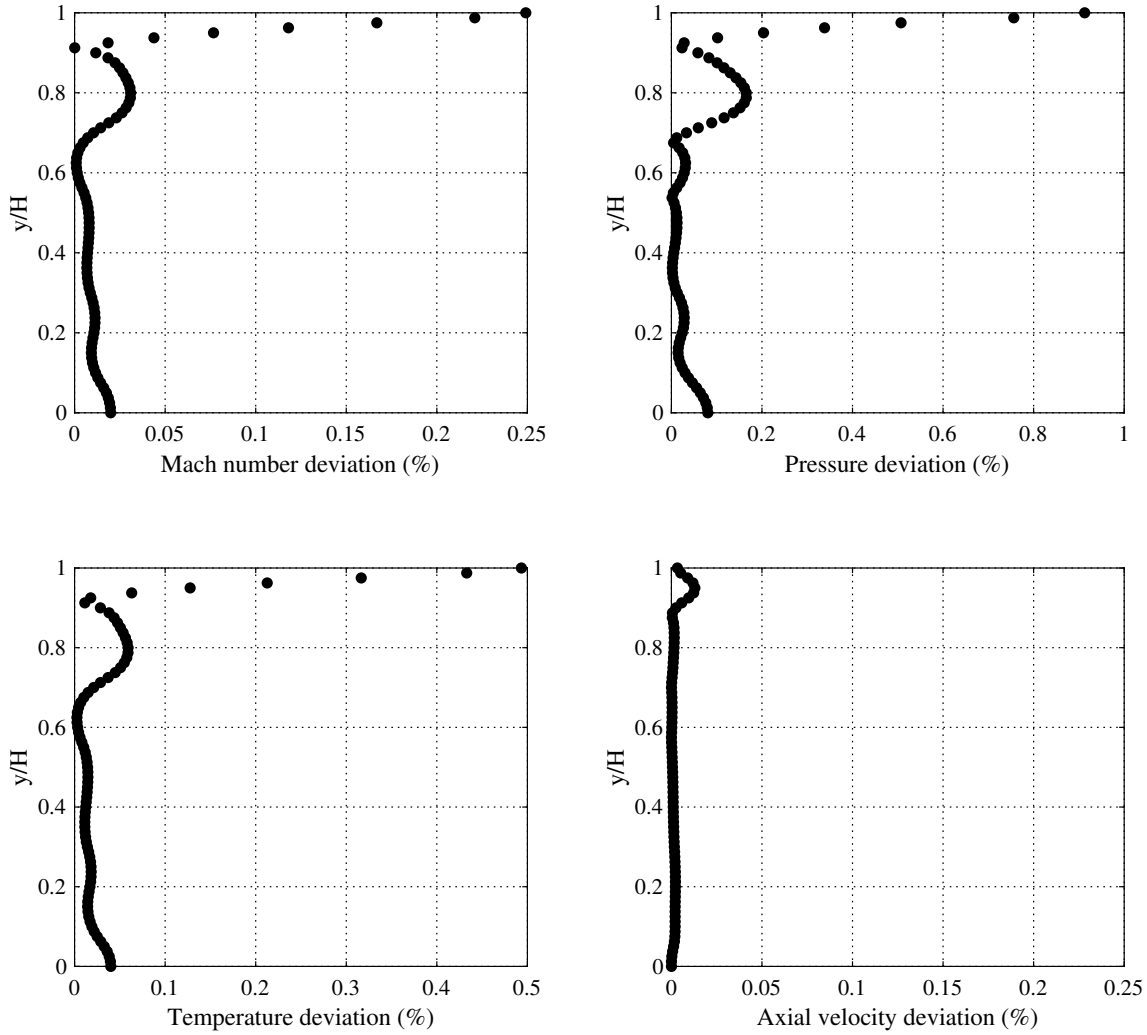

Figure 4.11: Axisymmetric Mach 9 nozzle exit plane property variation.

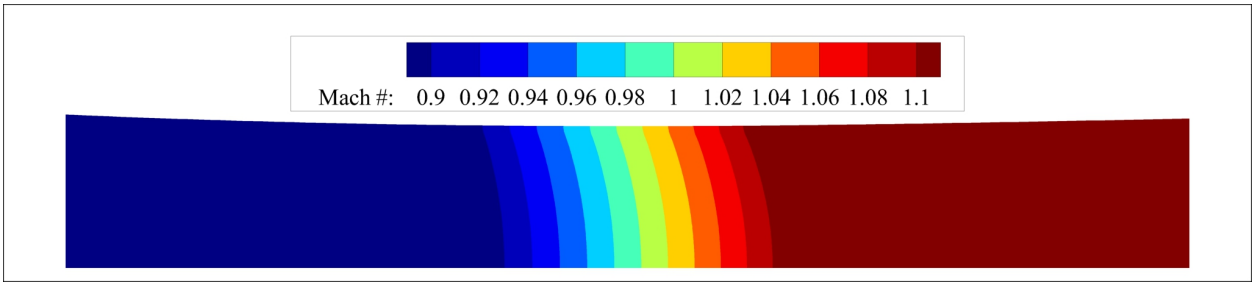

Figure 4.12: Axisymmetric Mach 9 nozzle throat.

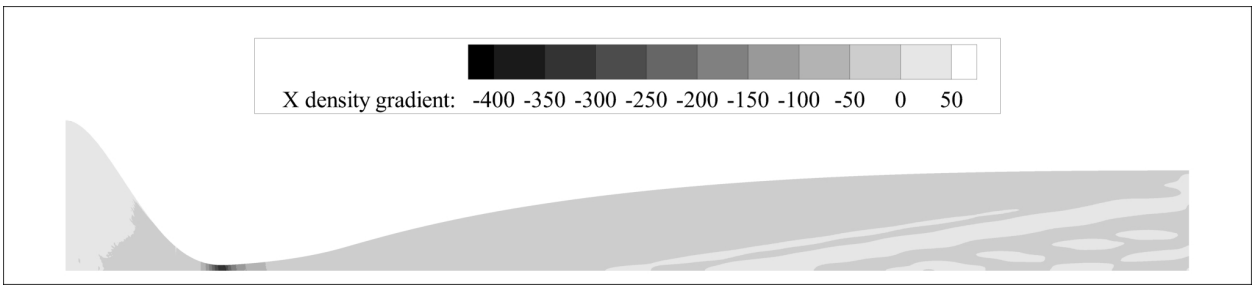

Figure 4.13: Axisymmetric Mach 9 nozzle X density gradient.

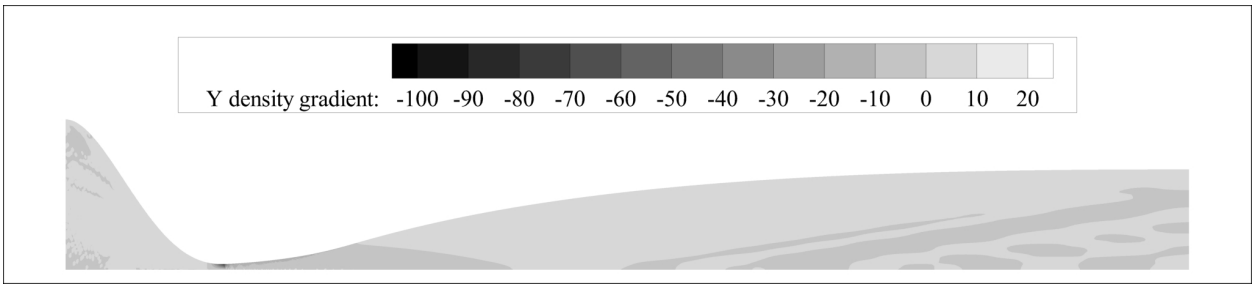

Figure 4.14: Axisymmetric Mach 9 nozzle Y density gradient.

4.3.4 Axisymmetric Mach 5.5 to Mach 7.5 Diverging Nozzle

Facilities such as the Hypervelocity Expansion Tunnel (HXT) at the National Aerothermochemistry & Hypersonics Labratory are built with a diverging nozzle to expand the test time of the core flow. A converging nozzle section is not needed in this type of facility because an unsteady expansion accelerates the flow to the supersonic speeds before the nozzle. To prove the design capabilities of the code for this type of nozzle, test conditions from a recent run in HXT were taken and used as initial conditions for the MOC code to expand the flow from Mach 5.5 to Mach 7.5. Figure 4.15 depicts the diverging nozzle achieving the design Mach number at the exit. The exit Mach line and transverse velocity are presented in Figures 4.16 and 4.17, and the property deviations at the exit plane are presented in Figure 4.18. Pressure fluctuations deviate slightly above the

definition for uniform flow, but these occur outside of the core flow region. The X and Y density gradients are presented in Figures 4.19 and 4.20.

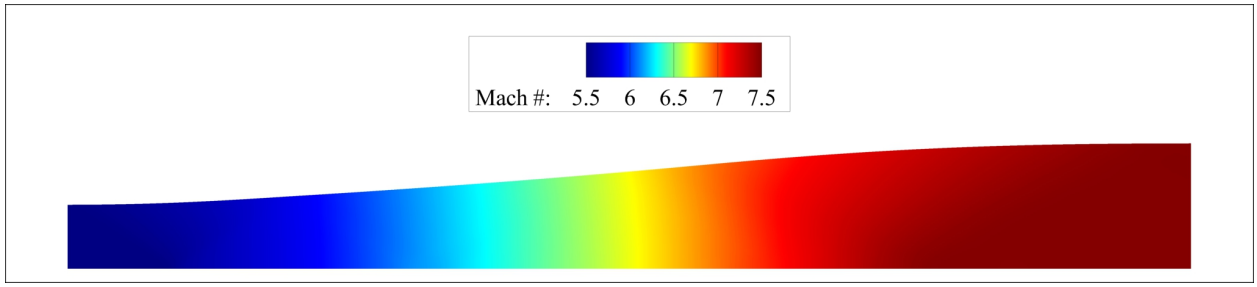

Figure 4.15: Axisymmetric Mach 5.5 to Mach 7.5 nozzle full-view.

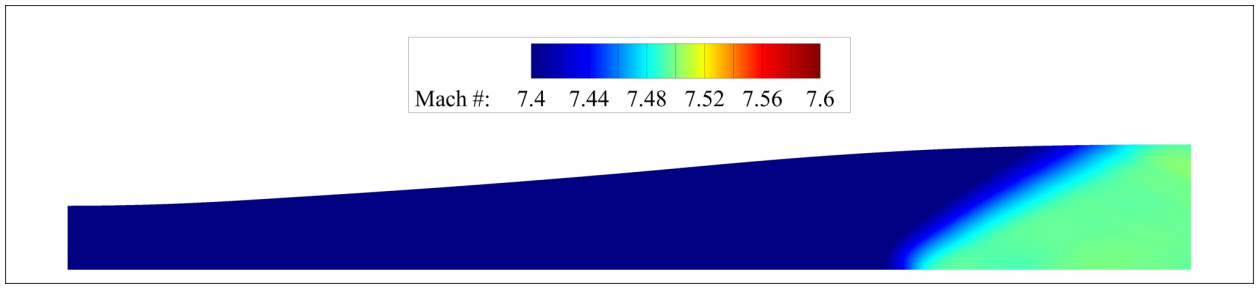

Figure 4.16: Axisymmetric Mach 5.5 to Mach 7.5 nozzle exit Mach line.

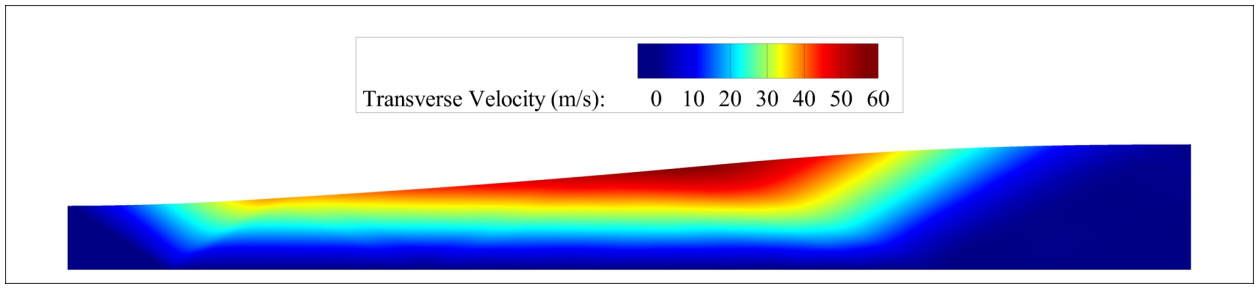

Figure 4.17: Axisymmetric Mach 5.5 to Mach 7.5 nozzle transverse velocity.

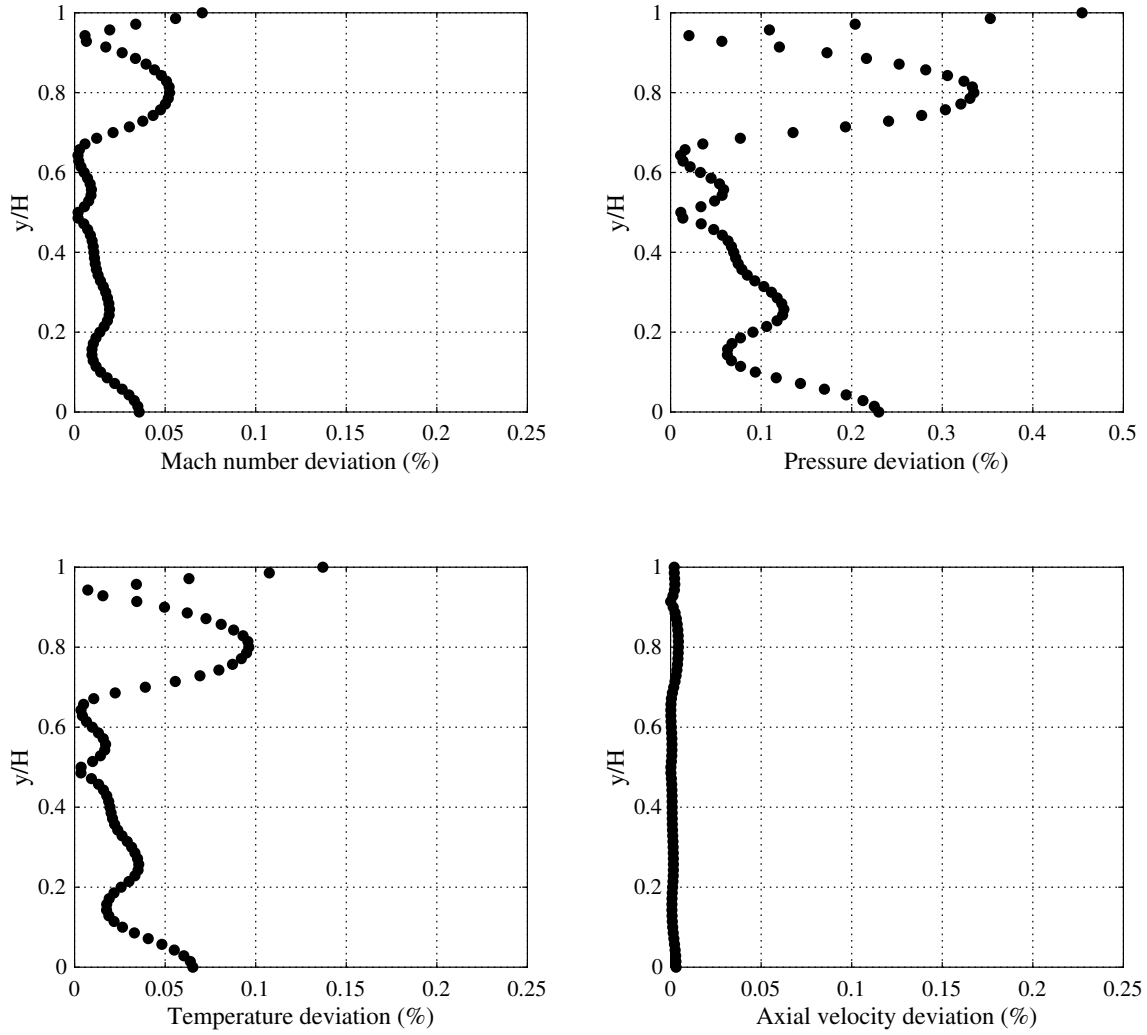

Figure 4.18: Axisymmetric Mach 5.5 to Mach 7.5 nozzle exit plane property variation.

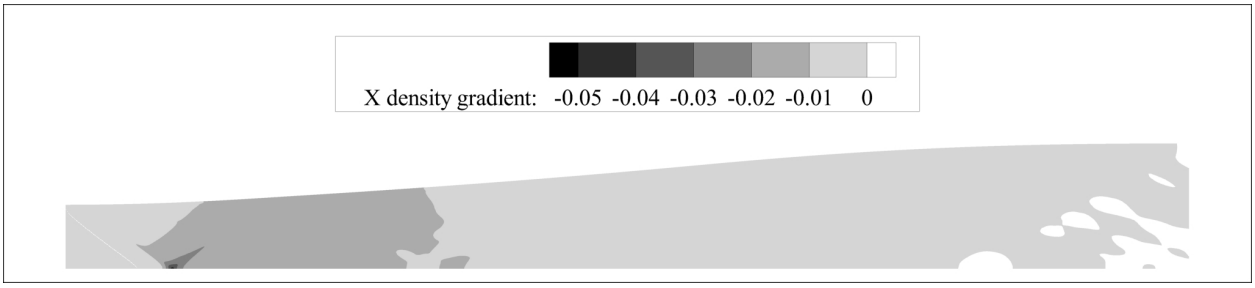

Figure 4.19: Axisymmetric Mach 5.5 to Mach 7.5 nozzle X density gradient.

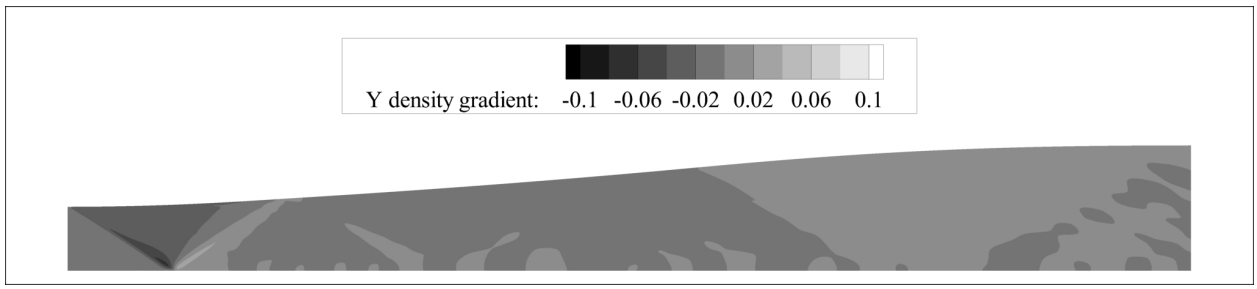

Figure 4.20: Axisymmetric Mach 5.5 to Mach 7.5 nozzle Y density gradient.

4.3.5 Planar Mach 5.5 to Mach 7.5 Diverging Nozzle

A planar diverging nozzle expanding flow from Mach 5.5 to Mach 7.5 was simulated to demonstrate the ability to model both axisymmetric and planar diverging nozzles. The same conditions from the axisymmetric case were used in this simulation. Figure 4.21 shows the full expansion of the flow. Figure 4.22 depicts the uniform flow delivered to the test section, and flow property variation at the exit plane is illustrated in Figure 4.23. Density gradients for the selected nozzle are presented in Figures 4.24 and 4.25.

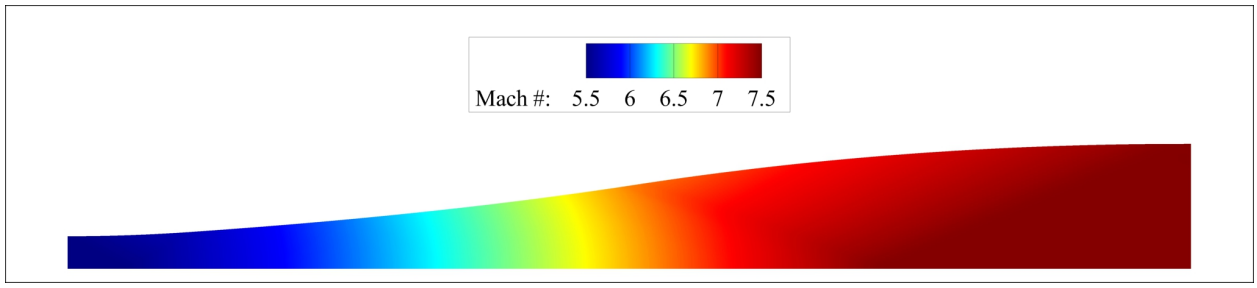

Figure 4.21: Planar Mach 5.5 to Mach 7.5 nozzle full-view.

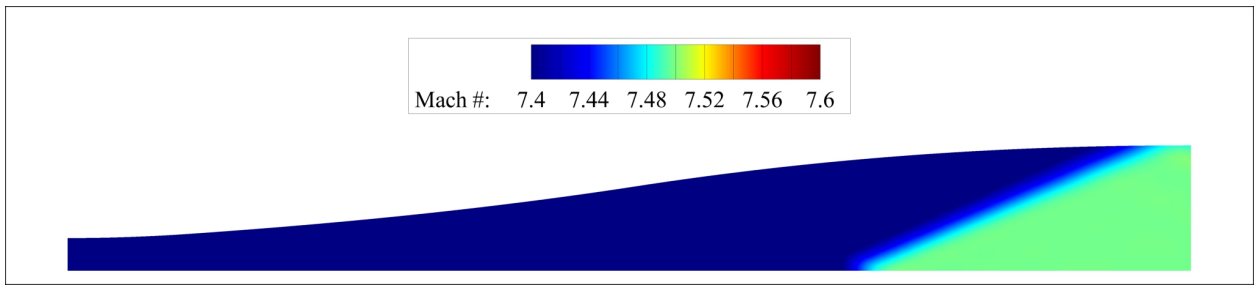

Figure 4.22: Planar Mach 5.5 to Mach 7.5 nozzle exit Mach line.

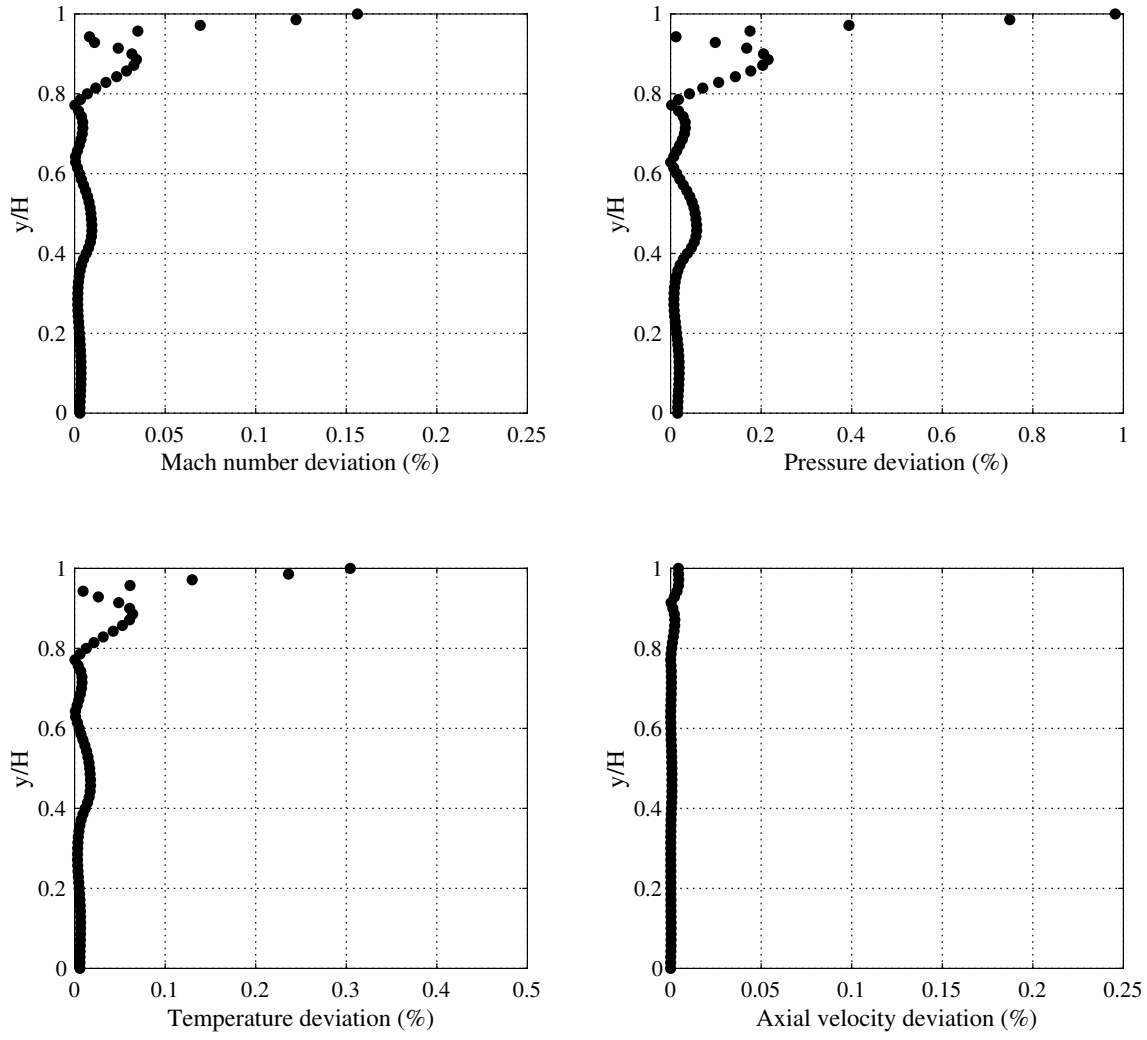

Figure 4.23: Planar Mach 5.5 to Mach 7.5 nozzle exit plane property variation.

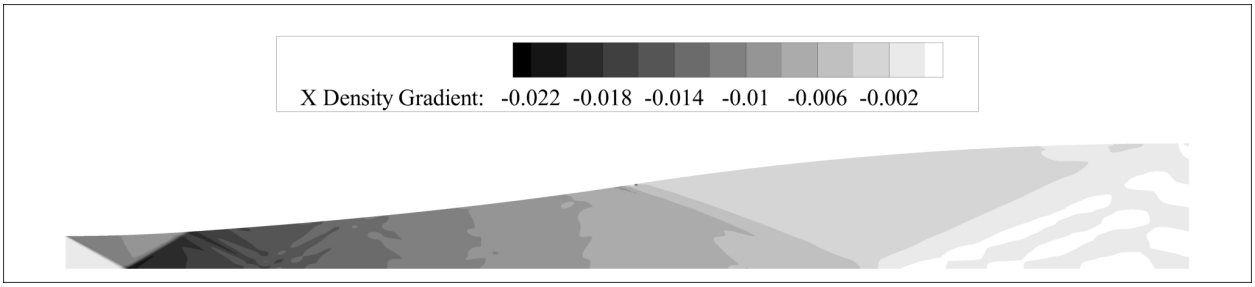

Figure 4.24: Planar Mach 5.5 to Mach 7.5 nozzle X density gradient.

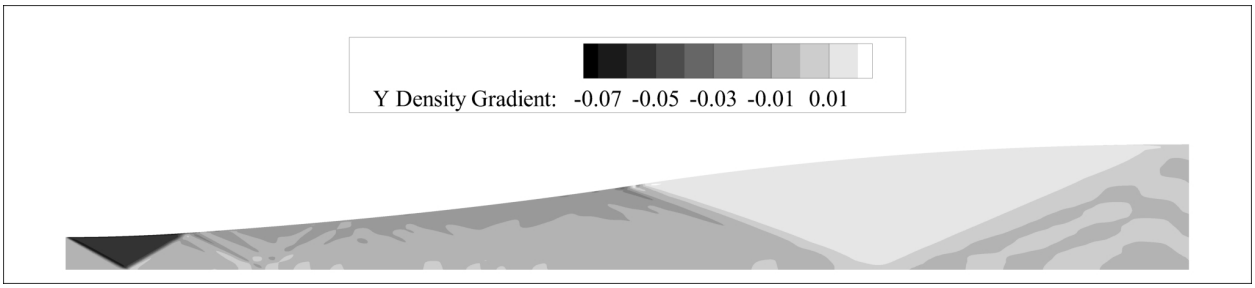

Figure 4.25: Planar Mach 5.5 to Mach 7.5 nozzle Y density gradient.

4.3.6 Planar Mach 5 Short, Medium, & Long Converging-Diverging Nozzles

The MOC code was developed to provide greater flexibility in the design parameters of a nozzle compared to current capabilities. To demonstrate this capability, a short, medium, and long Mach 5 nozzle were generated. The contours were superposed to each other for comparison, presented in Figure 4.26. Successful simulations for the three nozzle contours are presented in Figure 4.27.

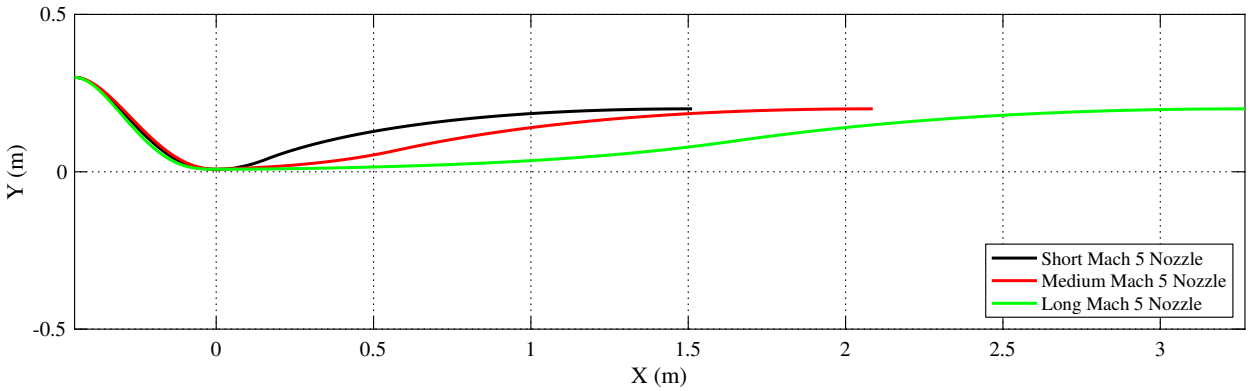

Figure 4.26: Planar Mach 5 nozzle extension comparison.

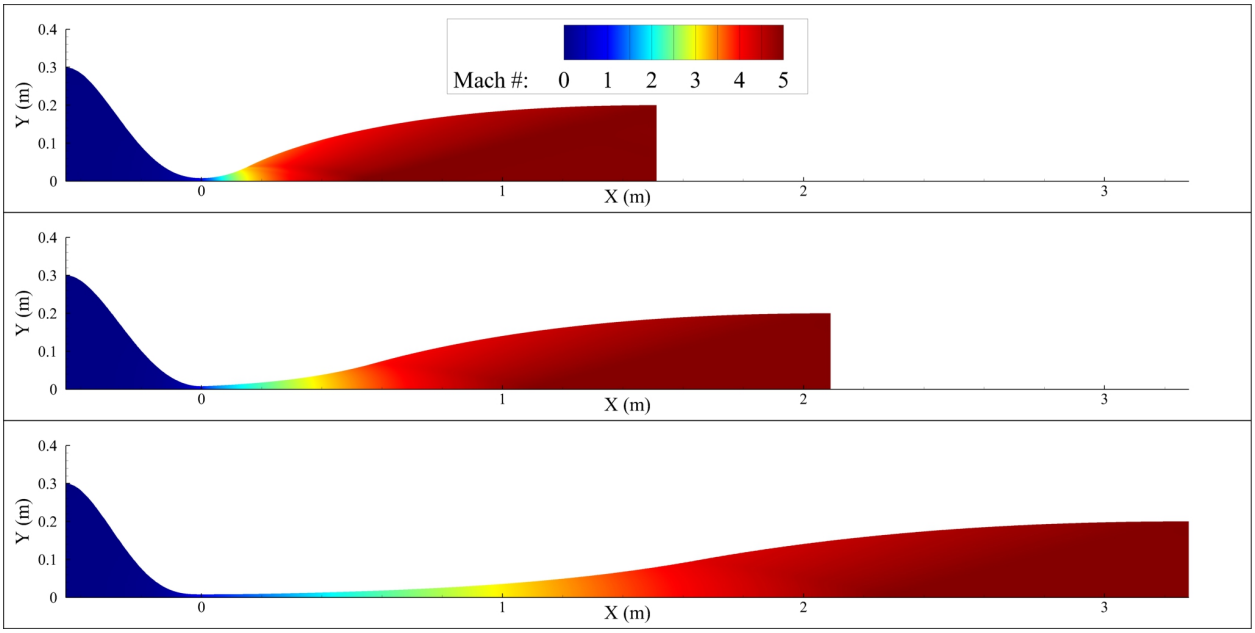

Figure 4.27: CFD solution for three Mach 5 nozzle contours.

5. CONCLUSIONS AND RECOMMENDATIONS

The purpose of this work was to develop a method of characteristics code to expand the capabilities of the National Aerothermochemistry and Hypersonics Laboratory. This was achieved by following the method of Zucrow & Hoffman ([31],[32]), modified to achieve the design Mach number on every design iteration.

5.1 Conclusions

Multiple test cases were simulated using US3D, including an axisymmetric Mach 9 converging-diverging nozzle, planar and axisymmetric diverging nozzles expanding Mach 5.5 to Mach 7.5, and planar Mach 5 short and long nozzles. Aerodynamically-uniform flow within defined limits was achieved at the exit plane for all test cases. It was determined that these results qualify the MOC code as successful.

5.2 Recommendations

Works by Benton, Candler, and Chan described the limitations of the MOC/BL method above Mach 8. Coupling a CFD solver with an optimization algorithm to improve the MOC/BL solution was shown to produce more uniform flow at the exit plane for Mach numbers from 4 up to 10. It is recommended to develop this capability for future hypersonic nozzles that operate above Mach 8.

REFERENCES

[1] Anderson, J. D., *Introduction To Flight*, McGraw-Hill Book Company, 3rd ed., 1989.

[2] Anderson, J. D., *Fundamentals of Aerodynamics*, McGraw-Hill Book Company, 5th ed., 2011, doi: 10.1017/s000192400000676x.

[3] Prandtl, L. and Busemann, A., "Naherungsverfahren zur Zeichnerischen Ermittlung von Ebenen Strömungen mit Übershllgeschwindigkeit," 1929.

[4] Crown, J. C., "Supersonic Nozzle Design," Tech. Rep. AD No. 62509, U.S. Naval Ordance Laboratory, 1950.

[5] Yu, Y.-N., "A Summary of Design Techniques for Axisymmetric Hypersonic Wind Tunnels," Tech. rep., North Atlantic Treaty Organization Advisory Group for Aeronautical Research and Development, 1958.

[6] Sivells, J. C., "Aerodynamic Design of Axisymmetric Hypersonic Wind Tunnel Nozzles," *AIAA 4th Aerodynamic Testing Conference*, 1969, doi: 10.2514/6.1969-337.

[7] McCabe, A., "Design of a Supersonic Nozzle Design of a Supersonic Nozzle," Tech. Rep. No. 3440, Univeristy of Manchester Aeronautical Research Council, London, 1964.

[8] Prince, D. C., "The Method of Characteristics for Supersonic Flow Analysis - A Fresh Perspective," *AIAA/ASME 3rd Joint Thermophysics, Fluids, Plasma and Heat Transfer Conference*, 1982, doi: 10.2514/6.1982-996.

[9] Wolf, S. W. D., "Supersonic Wind Tunnel Nozzles," Tech. rep., MCAT Institute, Moffett Field, 1990.

[10] Hartfield, R. J. and Burkhalter, J. E., "A Complete and Robust Approach to Axisymmetric Method of Characteristics for Nozzle Design," *51st AIAA/SAE/ASEE Joint Propulsion Conference*, 2015, doi: 10.2514/6.2015-4217.

[11] Evvard, J. C. and Marcus, L. R., "Achievement of Continuous Wall Curvature in Design of Two-Dimensional Symmetrical Supersonic Nozzles," Tech. rep., NACA, Cleveland, 1952.

[12] Yen, J. C. and Martindale, W. R., "An Inviscid Supersonic Nozzle Design Approach to Perfect Flow Uniformity for Wind Tunnel Applications," *26th AIAA Applied Aerodynamics Conference*, 2008, doi: 10.2514/6.2008-7059.

[13] Östlund, J. and Muhammad-Klingmann, B., "Supersonic Flow Separation with Application to Rocket Engine Nozzles," *Applied Mechanics Reviews*, Vol. 58, No. 1-6, 2005, pp. 143–176, doi: 10.1115/1.1894402.

[14] Goeing, M., "Nozzle Design Optimization by Method-of-Characteristics," *AIAA/SAE/ASME/ASEE 26th Joint Propulsion Conference*, 1990, doi: 10.2514/6.1990-2024.

[15] Young, R. B. and Hartfield, R. J., "Automated Nozzle Design through Axis-Symmetric Method of Characteristics Coupled with Chemical Kinetics," *48th AIAA/ASME/SAE/ASEE Joint Propulsion Conference and Exhibit*, 2012, doi: 10.2514/6.2012-4162.

[16] Kliegel, J. R. and Levine, J. N., "Transonic Flow in Small Throat Radius of Curvature Nozzles," *AIAA Journal*, Vol. 7, No. 7, 1969, pp. 1375–1378, doi: 10.2514/3.5355.

[17] Hopkins, D. F. and Hlll, D. E., "Effect of Small Radius of Curvature on Transonic Flow in Axisymmetric Nozzles," *AIAA Journal*, Vol. 4, No. 8, 1966, pp. 1337–1343, doi: 10.2514/3.3674.

[18] Rakich, J. V., "A Method of Characteristics for Steady Three-Dimensional Supersoinc Flow With Application to Inclined Bodies of Revolution," Tech. rep., National Aeronautics and Space Administration, Moffett Field, 1969.

[19] Jegede, O. O. and Crowther, W. J., "Low Order Supersonic Nozzle Design using Superimposed Characteristics," *54th AIAA Aerospace Sciences Meeting*, 2016, doi: 10.2514/6.2016-0805.

[20] Benton, J. R., Edwards, A. C., and Perkins, J. N., "Limitations of the Methods of Characteristics When Applied to Axisymmetric Hypersonic Nozzle Design," *28th Aerospace Sciences Meeting*, 1990, doi: 10.2514/6.1990-192.

[21] Candler, G. V. and Perkins, J. N., "Effects of Vibrational Nonequilibrium on Axisymmetric Hypersonic Nozzle Design," *29th Aerospace Sciences Meeting*, 1991, doi: 10.2514/6.1991-297.

[22] Korte, J. J., "Aerodynamic Design of Axisymmetric Hypersonic Wind-Tunnel Nozzles Using a Least-Squares/Parabolized Navier-Stokes Procedure," *Journal of Spacecraft and Rockets*, Vol. 29, No. 6, 1992, pp. 870–871, doi: 10.2514/3.55647.

[23] Korte, J. J., Kumar, A., Singh, D. J., and White, J. A., "CAN-DO, CFD-Based Aerodynamic Nozzle Design & Optimization Program for Supersonic/Hypersonic Wind Tunnels," *AIAA 17th Aerospace Ground Testing Conference, 1992*, 1992, doi: 10.2514/6.1992-4009.

[24] Korte, J. J. and Hodge, J. S., "Flow Quality of Hypersonic Wind-Tunnel Nozzles Designed Using Computational Fluid Dynamics," *Journal of Spacecraft and Rockets*, Vol. 32, No. 4, 1995, pp. 569–580, doi: 10.2514/3.26655.

[25] Shope, F. L., "Contour Design Techniques For Super/Hypersonic Wind Tunnel Nozzles," *24th Applied Aerodynamics Conference*, 2006, doi: 10.2514/6.2006-3665.

[26] Chan, W. Y., Jacobs, P. A., Smart, M. K., Grieve, S., Craddock, C. S., and Doherty, L. J., "Aerodynamic Design of Nozzles with Uniform Outflow for Hypervelocity Ground-Test Facilities," *Journal of Propulsion and Power*, Vol. 34, No. 6, 2018, pp. 1467–1478, doi: 10.2514/1.B36938.

[27] Sivells, J. C., "A Computer Program for the Aerodynamic Design of Axisymmetric and Planar Nozzles for Supersonic and Hypersonic Wind Tunnels," Tech. rep., Arnold Engineering Development Center, Arnold Air Force Station, 1978.

[28] Adams, S. E., *The Design and Computational Validation of a Mach 3 Wind Tunnel Nozzle Contour*, Master of science, University of Tennessee, Knoxville, 2016.

[29] Yoshio, D. and Uyeki, K., *A Design Method for a Supersonic Axisymmetric Nozzle for Use in Wind Tunnel Facilities*, Master of science, San Jose State Univeristy, 2018.

[30] Anderson, J. D., *Modern Compressible Flow With Historical Perspective*, McGraw-Hill Book Company, 3rd ed., 1983, doi: 10.1016/0142-727x(83)90029-2.

[31] Zucrow, M. J. and Hoffman, J. D., *Gas Dynamics Volume I*, John Wiley & Sons, Inc., 1976.

[32] Zucrow, M. J. and Hoffman, J. D., *Gas Dynamics Volume II*, John Wiley & Sons, Inc., 1977, doi: 10.1213/01.ane.0000492743.10184.13.

[33] Candler, G. V., Johnson, H. B., Nompelis, I., Subbareddy, P. K., Drayna, T. W., Gidzak, V., and Barnhardt, M. D., "Development of the US3D code for advanced compressible and reacting flow simulations," *53rd AIAA Aerospace Sciences Meeting*, 2015, doi: 10.2514/6.2015-1893.

[34] Shope, F. L., "Design Optimization of Hypersonic Test Facility Nozzle Contours Using Splined Corrections," Tech. rep., Arnold Engineering Development Complex, 2005.